Design and Construction of a Slotted Coaxial Balun and the Development of a Method to Determine Noise Temperature of LNAs with Non Standard Input Impedances.

Simon B. Nawrot
ATNF vacation student
February 2003

Abstract

This paper outlines the design and construction of a system similar to what may be connected between a proposed zigzag antenna and the first LNA in an element of an SKA adopting the Luneburg Lens approach. It is also the objective of this paper to outline a procedure by which the noise temperature of candidate LNAs and the first stage matching for the SKA can be measured. The procedure described has been specifically designed so that the noise temperature of LNAs with non standard input impedances can be measured. The 50Ω connections required by commercial noise figure meters do not allow for a non standard impedance.

Introduction

CSIRO's SKA team are investigating the increase in thermal noise performance of an uncooled front end operating with a non standard input impedance other than 50Ω [1]. The paper outlines the design and construction of a possible front end system operating between 1 and 5 GHz that is able to provide a transformation from a 200Ω unbalanced termination required by the antenna to a 50Ω balanced termination required by a standard LNA. The resulting system is a balun/taper combination. The 50Ω termination was used for this prototype, however, transformation to a non standard impedance can be achieved by following the same method. The performance has been tested and results are presented.

The paper also outlines a procedure by which the noise temperature of an LNA or balun/taper/LNA combination can be measured. It is recommended that the system as outlined in this paper be used to measure the noise temperature when an LNA of standard 50Ω impedance is used. This will allow the measurement procedure to be evaluated. The system will be used in two situations. The first situation will allow the system to connect to an experimental antenna. The second situation will allow for connection to a resistor that will be used as a hot/cold thermal noise source for noise temperature measurement. This paper will concentrate on the latter situation

Description of required System

The System

The system will be used in two different situations. These are the Field Measurement situation in which the system is connected to an experimental zigzag antenna and the Bench Measurement situation in which the system is connected to a resistor.

The field measurement system will provide a means by which the performance of the proposed front end can be tested. It will also provide a means by which noise figure will be measured as the zigzag antenna is directed at hot and cold sources.

The bench measurement system has been constructed. By heating and cooling a thin film chip resistor acting as a noise source, noise power measurements can be taken and then by using the Y factor method [9], noise temperature can be calculated.

Both systems are similar in that they are both initially required to transform the 200 ohm antenna impedance down to the standard 50 ohms required by a standard LNA. Both systems also require a balun so that the balanced termination required by the antenna can be transformed to the unbalanced coaxial termination required by an LNA.

Field Measurement

The field measurement apparatus consists of:

i) A broadband zigzag antenna as the noise source,
ii) an LNA as the device under test,
iii) a coaxial 'cutaway' balun to transform the balanced wire system from the antenna terminals to an unbalanced coaxial terminal required by the LNA,
iv) a taper to go between the antenna and balun terminals to provide the correct physical spacing and correct impedance match,
v) a power meter connected to the output of the LNA so that noise figure can be measured.

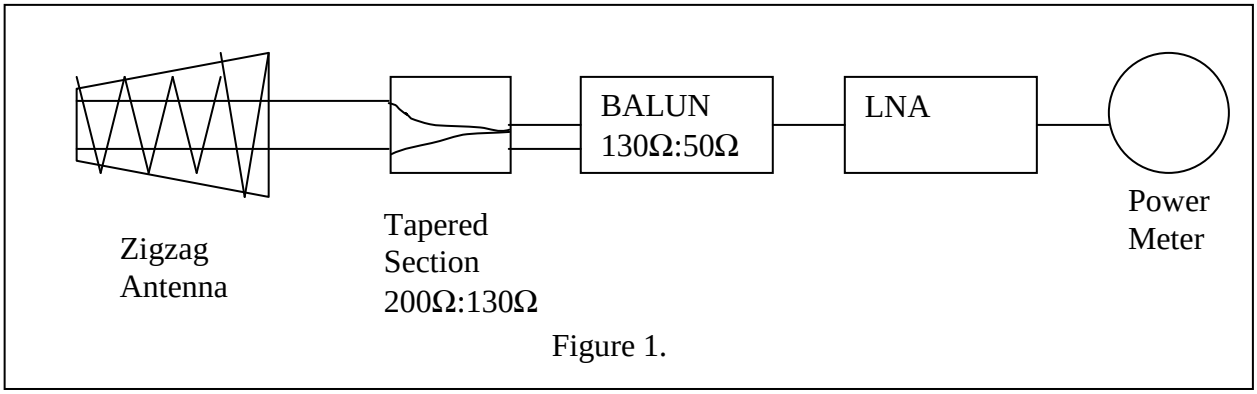

Figure 1.

Bench Measurement

The bench measurement apparatus consists of:

i) a chip of 180 ohms to act as the noise source and to simulate the zigzag antenna's impedance,
ii) an LNA as the device under test,
iii) the same 'cutaway' balun as used in the field measurement,
iv) a taper to go between the resistor and balun terminals to provide the correct physical spacing and correct impedance match,
v) the same power meter as used in the field measurement.

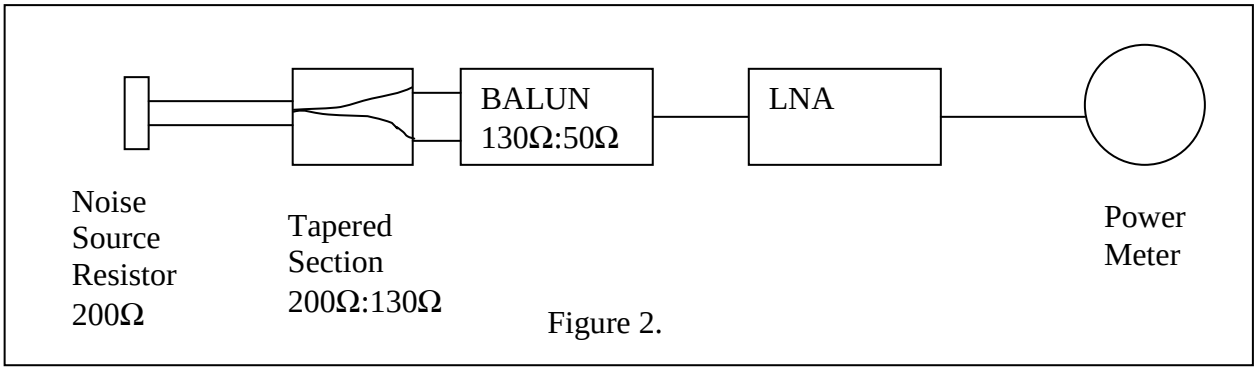

Figure 2.

Description and Design of System Components

Zigzag antenna

The antenna is broadband and covers the 1-5GHz frequency range of interest. The zigzag antenna is predicted to have a nominal input impedance of approximately 200 ohms. The input impedance of the antenna is expected to vary by a small amount in harmony with the periodicity of the zigzag structure as the frequency is varied. The main beam is axial to the antenna and radiates in the direction of its apex.

LNA

A commercially available LNA with 50 ohm input and output impedance will be used for initial testing. By later altering the impedance transformation, the system can be matched to the impedance required at the input of a non standard LNA to provide a means to measure its noise temperature.

Balun

The balun was constructed from of a piece of rigid 50Ω coax. The dielectric material has a dielectric constant of 1.5 that was determined from measurements of the cable's dimensions. The loss tangent is unknown. The cable has an outer conductor of aluminium and an inner conductor of copper.

Approximate dimensions are:
ID = 8.23mm,
OD = 9.6mm,
Centre Conductor Diameter = 2.97mm,
Outer Conductor Thickness = 0.7mm.

The balun has two functions: to transform a balanced system to an unbalanced system and to provide some impedance transformation. This is achieved by cutting a slot in the coax and gradually widening the slot down its length until two parallel balanced conductors remain with the height of the remaining shield being equal to the diameter of the centre conductor. At the end of the balun the slot angle is 323 degrees. Transition from a balanced to an unbalanced system is achieved by the tapered geometry of the slotted coax that ensures that all currents are gradually confined to the inside surface of the coax when the unbalanced terminal is reached [2].

The rate at which the slot is widened down the length of the coax is determined by the required characteristic impedance contour of the impedance transformation. The characteristic impedance contour is determined by the 'Klopfenstein Taper' [3] that is optimum in the sense that it has minimum reflection coefficient in its pass band for a specified length of taper.

The chosen length of the taper was 20cm and at the lowest frequency of 1 GHz this corresponds to 2/3 of a wavelength. With the balun incorporating the Klopfenstein taper the maximum expected reflection coefficient at frequencies above 1 GHz is 2.1%. Calculations for the Klopfenstein taper were performed using an iterative process on computer using the method in [4].

Determination of the characteristic impedance of slotted coax was determined from the design equations provided in [2]. The dielectric constant of 1.5 was substituted for the air permittivity that was used in the paper and a new set of design curves were drawn. An approximation was made here because the permittivity associated with the design equation is that of the entire environment surrounding the slotted coax and is not restricted to the coaxial dielectric. The effect of this approximation was modelled for the case where the field has the least containment i.e. at the end of the balun where the slot angle is 323 degrees. The difference in characteristic impedance between the case where the dielectric filled the entire environment and the case where the dielectric was restricted to the coaxial dielectric was only 7 ohms. This was not considered significant and the approximation was deemed satisfactory.

The required Klopfenstein Taper and the impedance of the slotted coaxial cable are given in the figure 3 and 4 respectively.

Figure 3.

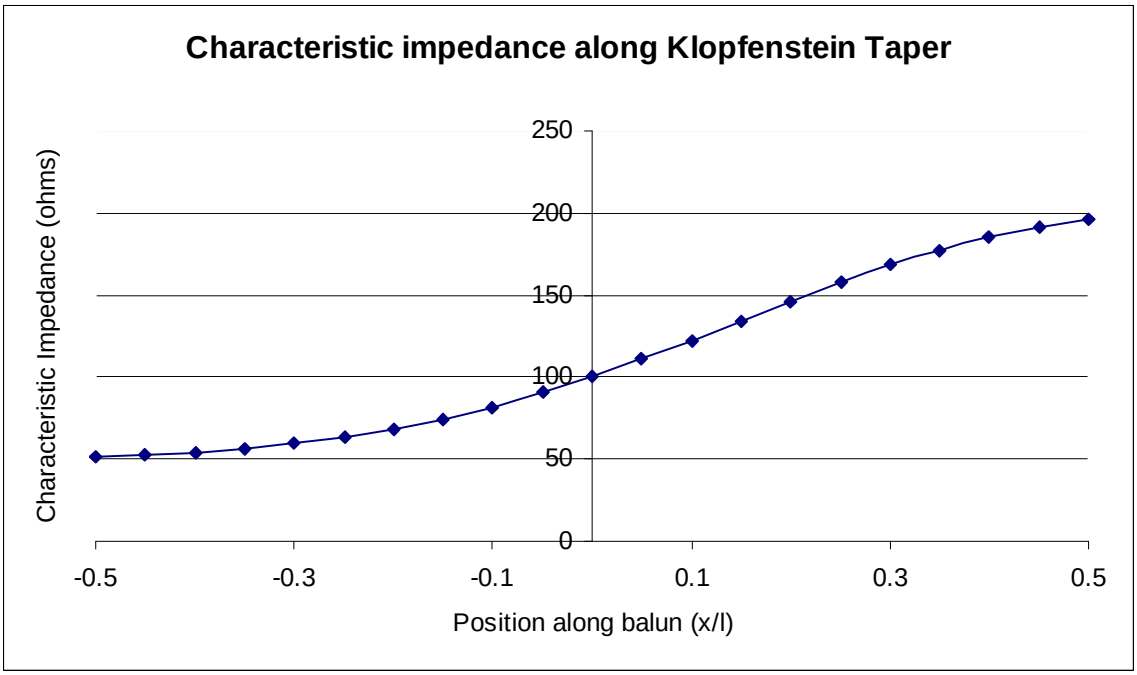

Figure 4.

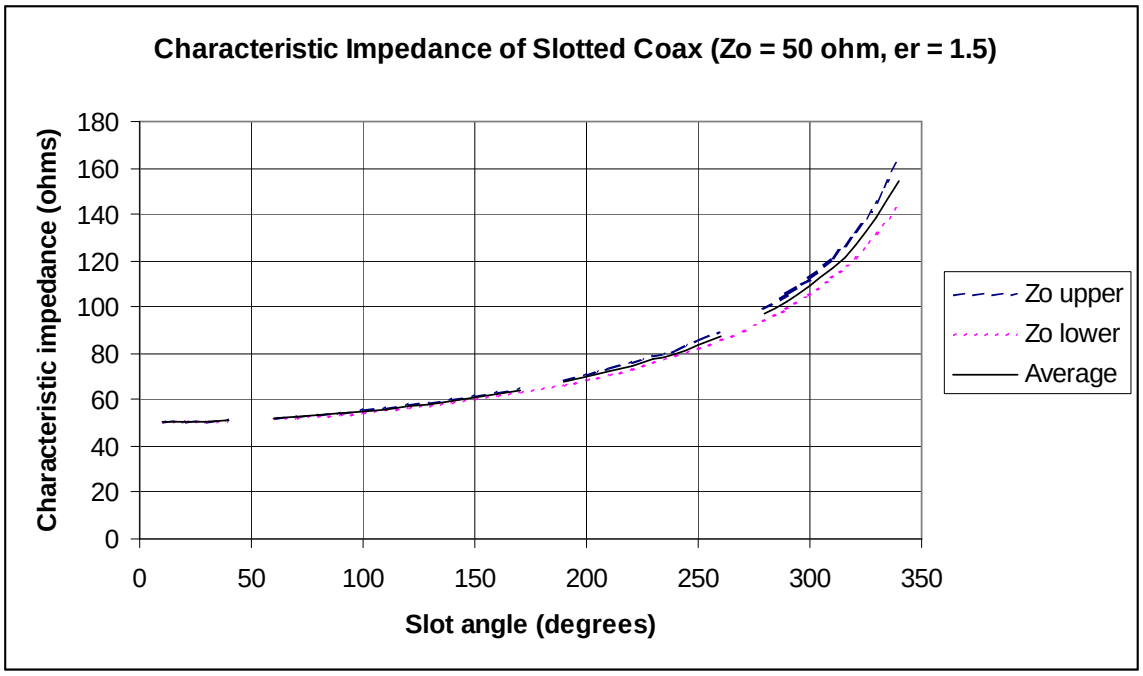

From the curves it can be seen that with a slot angle of 323 degrees the characteristic impedance is 130 ohms, however, the required impedance at the antenna is 200 ohms. In order to transform from 50 to 200 ohms it is necessary to continue the Klopfenstein taper into the tapered section between the balun and resistor. i.e. The balun will contain that part of the impedance contour between 50 and 130 ohms and the tapered section will contain that part of the impedance contour between 130 and 200 ohms. This corresponds to the balun containing the first 127mm of the taper. The function of the slot angle with respect to the distance along the balun is approximated as two linear sections and was determined from a combination of the results shown in Figure 3 and Figure 4. This is shown in figure 5.

Figure 5.

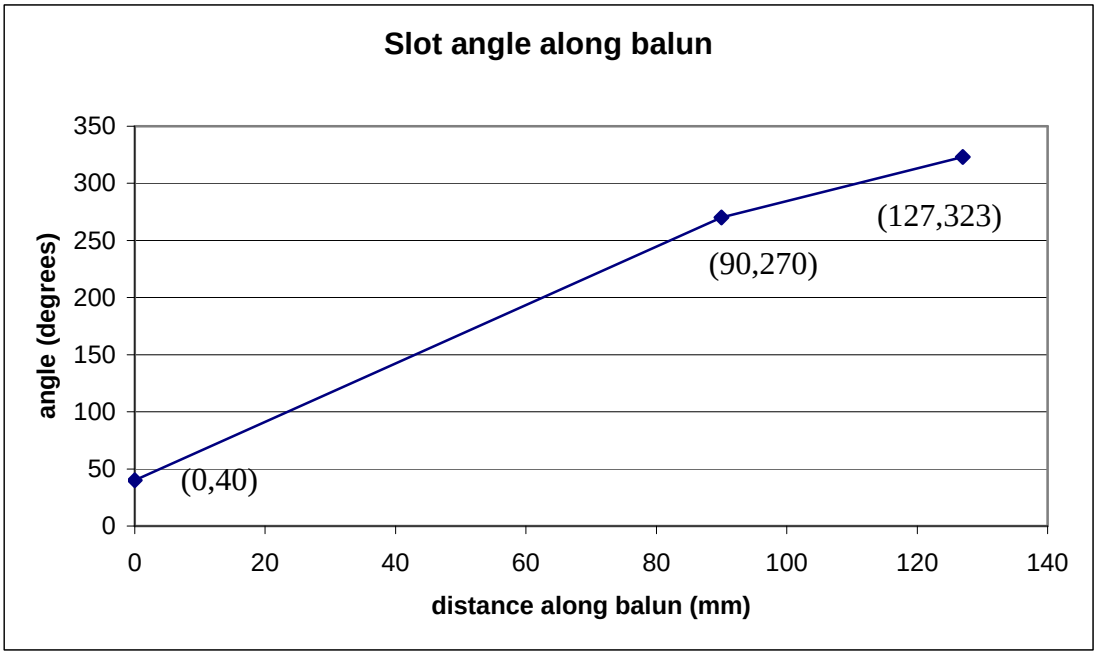

The design drawing of the balun is shown in Appendix A.

Construction

To cut away the slot in the coax a number of different construction techniques were attempted. Some had more success than others.

To cut away the slot in the coax, one chosen method was to etch the required pattern with hydrochloric acid. A template was made on a piece of paper and this was wrapped around the cable so that the pattern could be scribed on the surface with a knife. A number of methods to mask the desired portion of the cable were tried with varying levels of success.

The first method attempted involved dipping the cable in molten wax. The pattern that was previously scribed on the cable was still visible through the wax and this allowed the removal of the wax with a small knife. With the undesired portion of the aluminium now exposed the cable was then immersed in 33% hydrochloric acid solution. This method, however, was unsuccessful. The principal reason being that the localised heating generated by the reaction caused the wax to soften and this resulted in unacceptable under etching and in some cases, complete destruction of the mask.

Other masking materials were tried. Flexible PVC tape was tried, however, localized heating also caused the tape to come away at the edges, although in some places the etch was very clean. It is thought that using a weaker acid solution may produce better results in this case. Other masking materials tried were Dulux flat black enamel spray paint and photographic resist. Before coating an outline of the required slot was masked on the coax with 1.27mm crepe masking tape. The enamel paint was applied by spraying and the photographic resist was applied by dipping. In both cases after coating, the tape was removed to expose bare aluminium in the shape of the slot perimeter. In the case where the photographic resist was used, the balun was baked at approximately 80°C for about one hour in an attempt to harden the coating. Unfortunately the masking material in both cases was destroyed through the etching process. The enamel paint flaked off in sections and the photographic resist withstood the acid for some time before destruction. It is thought, however, that air bubbles in the resist coating may have been a contributing factor to its failure. It may be possible that good results can be achieved if the photographic resist is brushed on to provide a thinner more uniform coating.

Other surface coatings for use as a mask may need to be tried in future. A bituminous type paint has been suggested.

Figure 6 – Some failed etching attempts. The black coating is enamel paint, the red coating is photographic resist.

The balun that has been produced was constructed using a paper template that was wrapped around the cable. Exposed aluminium was then removed carefully using a rough bladed hacksaw and any excesses removed by filing. Care was taken to minimise damage to the dielectric material during cutting.

Chip Resistor

The resistive termination consists of a 180Ω thin film chip resistor. The resistor is 'State of the Art' size SO402 approximately corresponding to dimensions of 0.25mm x 0.5mm. The resistor is mounted on the end of the taper on the PCB.

Taper from balun to chip resistor

The taper from balun to chip resistor consists of two parallel plates etched on a single sided PCB with 0.762mm substrate thickness and 17um conductor thickness (Rogers RT duroid 6002). Dielectric constant is 2.94 and loss tangent 0.0012. The taper provides a reduction in conductor spacing from 3mm at the balun terminal down to 1mm at the chip resistor. The taper also provides the remainder of the Klopfenstein impedance contour from 130 to 200 ohms. At the interface between the balun and the PCB the two parts were soldered together. This rapid transition did have some effect on the system performance but satisfactory results were still obtained.

Design of the taper

The PCB taper is supposed to provide that part of the Klopfenstein taper between 130Ω and 200Ω. For this requirement the taper is 7.35 cm long. A number of points along the taper were defined. The positions of these points are shown in figure 7 below.

Figure 7.

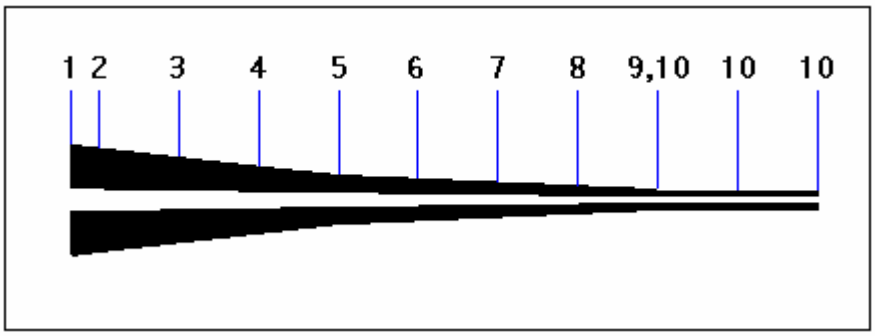

From the results displayed in figure 3 the required impedances along the taper are shown in Table 1.

Table 1.

Point no.	Distance from pt.1 (cm)	Required Z
1	0	130
2	0.35	134
3	1.35	146
4	2.35	158
5	3.35	168
6	4.35	178
7	5.35	186
8	6.35	191
9	7.35	196
10	Termination	200

To determine the correct track widths and spacing a finite difference two dimensional (FD2D) field solving program was used [5]. The program allowed the entry of a two dimensional cross section of an arbitrary line into its graphical interface. This allowed the geometry of the substrate and conductors to be specified. The required characteristic impedance at each point along the taper was obtained by varying the width and spacing of the tracks by trial and error. The results obtained by the program are shown in Table 2.

Table 2.

point no.	Z obtained	L (uH/m)	C (pF/m)	V ($\times 10^8 m/s$)	W (mm)	s (mm)
1	130	0.5027	29.85	2.58	6.7	3
2	136	0.55	29.7	2.57	5	2.9
3	148	0.5853	26.42	2.54	4	2.6
4	161	0.62	23.9	2.48	3	2.3
5	169	0.6846	25.22	2.41	2	2
6	178	0.757	23.88	2.35	1.6	1.75
7	187	0.7887	22.63	2.37	1.25	1.5
8	193	0.8239	22.04	2.35	1	1.25
9	195	0.8514	22.59	2.28	0.7	1
10	201	0.8884	21.96	2.26	0.62	1

Where:
L is the distributed inductance,
C is the distributed capacitance,
v is the velocity of propagation,
W is the width of the tracks and,
s is the spacing between tracks.

Construction of the Taper

The Taper was photographically etched on a 100mm x 40 mm piece of Rogers RT Duroid 6002 board. The mask required for etching was drawn in Solidworks and printed black onto a transparency sheet with a colour printer.

Calculating the Loss in the PCB Taper

In order to determine the loss in the PCB taper it is necessary to form some equations for the loss in terms of the variables provided by the FD2D program in Table 2. The total loss of the PCB taper is contributed to by the dielectric loss and the conductor loss. From [6], the attenuation constant in dB/metre is given by:

$$\alpha = \left(4.34\frac{R}{Z_0} + 4.34GZ_0 \right) dB/m \qquad \text{…….(1)}$$

where:

R is the distributed resistance of the line in Ω/m,
G is the distributed conductance of the line in S/m,

$4.34\frac{R}{Z_0}$ is the conductor loss …….(1a)

$4.34GZ_0$ is the dielectric loss. …….(1b)

1. Calculation of the Distributed Resistance R

Equation (6.30) in [7] can be modified to suit the geometry of the cross section for the taper to give the distributed resistance of a single conductor:

$$R_{\sin gle} = \frac{R_s}{2W} \qquad \text{…….(2)}$$

where:

$$R_s = \frac{1}{\sigma\delta} = \sqrt{\frac{\pi f \mu_0}{2\sigma}}, \qquad \text{…….(2a)}$$

$\sigma = 58MS/m$ for copper,

μ_0 is the permeability of free space,

2W is twice the width of a track. i.e. The approximate cross sectional perimeter of the track is used in accordance with the above assumption.

Because there are two lines in the taper it is necessary to multiply $R_{\sin gle}$ in (2) by 2 and use the proximity factor P determined as in appendix 2 for the calculation of R:

$$R = \frac{R_s}{W} P \qquad \text{…….(3)}$$

Combining (2a) with (3) the required expression for R is obtained:

$$R = \frac{\sqrt{\frac{\pi f \mu_0}{2\sigma}}}{W} P \qquad \text{…….(4)}$$

2. Calculation of the distributed conductance G

From equation (3.10) in [6] the distributed conductance can be calculated by:

$$G = 2\pi f C \tan\delta_{eq} \qquad \text{…….(5)}$$

Where $\tan\delta_{eq}$ is the equivalent loss tangent at a point along the line i.e. it is a combination of the loss tangent of the air $\tan\delta_{air}$ =0, and the loss tangent of the substrate $\tan\delta_s$ that has the equivalent effect of a uniform dielectric at that point.

Equation (3.11) in [6] can be converted to a more arbitrary form useful for our purposes so that the equivalent loss tangent can be found in terms of $\tan\delta_s$, ε_s and ε_{eq}:

$$\tan\delta_{eq} = \frac{\varepsilon_s}{\varepsilon_{eq}}\left(\frac{\varepsilon_{eq}-1}{\varepsilon_s-1}\right)\tan\delta_s . \qquad \text{…….(6)}$$

Where:

ε_s is the dielectric constant of the substrate,

ε_{eq} is the equivalent dielectric constant at a point along the line. i.e. It is the combination of the air dielectric constant ε_{air} =1 and substrate dielectric constant ε_s at a point along the line that has the equivalent effect of a uniform dielectric at that point.

ε_{eq} can be determined if the velocity of propagation v at a point along the line is known.

$$\varepsilon_{eq} = \left(\frac{c}{v}\right)^2 \qquad \text{…….(7)}$$

Where c is the velocity of light.

Substituting (7) into (6) and then (6) into (5) the required expression in terms of $\tan\delta_s$, ε_s, and v is obtained:

$$G = \frac{2\pi f C\varepsilon_s\left(1-\left(\frac{v}{c}\right)^2\right)\tan\delta_s}{\varepsilon_s-1} \qquad \text{…….(8)}$$

3. Determination of Conductor Loss, Dielectric Loss, and Attenuation Constant

Substituting (4) into (1a) the conductor loss is obtained.

$$Loss_{conductor} = 4.34\frac{\sqrt{\frac{\pi f\mu_0}{2\sigma}}}{WZ_0}P \text{ (dB/metre)} \qquad \text{…….(9)}$$

Substituting (8) into (1b) the dielectric loss is obtained.

$$Loss_{dielectric} = 4.34Z_0\frac{2\pi f C\varepsilon_s\left(1-\left(\frac{v}{c}\right)^2\right)\tan\delta_s}{\varepsilon_s-1} \text{ (dB/metre)} \qquad \text{…….(10)}$$

Addition of (9) and (10) yields the total loss or the attenuation constant α in dB/metre.

$$\alpha = 4.34\left(\frac{1}{WZ_0}\sqrt{\frac{\pi f\mu_0}{2\sigma}}P + Z_0\frac{2\pi fC\varepsilon_s\left(1-\left(\frac{v}{c}\right)^2\right)\tan\delta_s}{\varepsilon_s - 1}\right) \text{(dB/metre)}$$

…….(11)

4. Results

To approximate the total loss of the taper, the taper was broken up into elements. Each element was assigned the data from a point as shown in figure 8 below:

Figure 8.

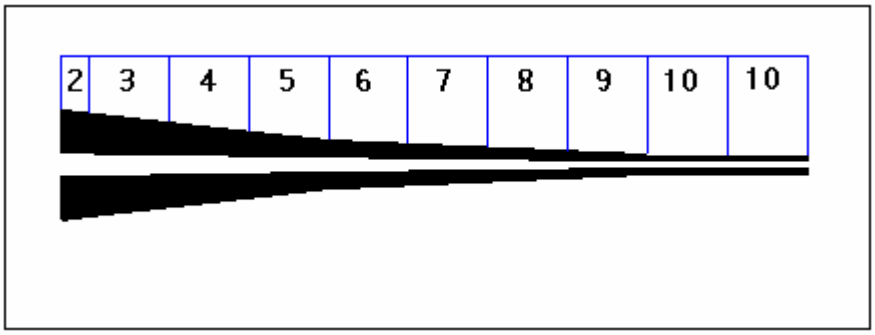

Numerical values of the required variables are given in Table 2. Some other required values are:

ε_s =2.94,

$\tan\delta_s$ =0.0012,

$\sigma = 58MS/m$,

$\mu_0 = 4\pi\times10^{-7}$,

$c = 3\times10^8 m/s$

Table 3 shows some intermediate results for the loss calculations. Results are given for each element in the taper. The proximity factor values were calculated as in Appendix 2.

Table 3.

Element no.	ε_{eq}	$\tan\delta_{eq}$	G/f $(S/m/GHz)$	P	$R/\sqrt{f}$ $(\Omega/m/Hz)$	Element Length (cm)	$Loss_{dielectric}$ (dB/GHz)	$Loss_{conductor}$ $(dB/\sqrt{Hz})$
2	1.36	0.000484	9.03E-05	1.91	9.98E-05	0.35	0.000187	1.11E-08
3	1.39	0.000512	8.5E-05	1.78	0.000117	1	0.000546	3.42E-08
4	1.46	0.000576	8.65E-05	1.83	0.000159	1	0.000604	4.29E-08
5	1.55	0.000649	0.000103	1.73	0.000226	1	0.000754	5.8E-08
6	1.63	0.000701	0.000105	1.75	0.000285	1	0.000812	6.95E-08
7	1.61	0.000686	9.76E-05	1.71	0.000358	1	0.000792	8.31E-08
8	1.63	0.000706	9.77E-05	1.67	0.000437	1	0.000818	9.83E-08
9	1.73	0.000768	0.000109	1.68	0.000627	1	0.000923	1.4E-07
10	1.76	0.000783	0.000108	1.58	0.000666	2	0.001885	2.88E-07
						total	**0.007321**	**8.24E-07**

Table 4 shows results for the Dielectric loss, Conductor loss, and total loss over the entire PCB taper for frequencies between 1 and 5 GHz. The final column gives an indication of a loss per unit length.

Table 4.

frequency (GHz)	Dielectric loss in PCB (dB)	Conductor Loss in PCB (dB)	Total Loss in PCB (dB)	dB/m
1	0.007	0.026	0.033	0.36
2	0.015	0.037	0.052	0.55
3	0.022	0.045	0.067	0.72
4	0.029	0.052	0.081	0.87
5	0.037	0.058	0.095	1.01

Note: In microstrip transmission lines it is normally expected that the dielectric loss will supercede the conductor loss at around the frequencies shown in table 4. This, however, is not the case in the results shown in Table 4 for an open wire PCB conductor geometry. There are three reasons for this:

i. The PC board has low loss.
ii. The geometry of the open wire line on the PCB means that a large proportion of the field is in air as well as in the PCB and this reduces the dielectric loss.
iii. The wide flat conductors of the line cause the currents to be less evenly distributed in the conductors and this results in an increased proximity factor and therefore increased conductor loss.

Modelling of the Heat Conduction when the noise source is heated and cooled

Concerns were raised in regard to the heating and cooling of the LNA as a result of heat conduction through the taper and balun when the noise source is heated and cooled. Recommendations were made that involved building a section of the taper from copper plated stainless steel that has a much lower thermal conductivity to act as a thermal barrier. The heat conduction was approximately modeled using Fourier's One Dimensional Heat Transfer Equation for a finite bar with fixed end temperatures [8].

Derivation of the model can be found in [8]. The model provides a conservative (worst case) indication of the heat distribution along the length 'x' of the taper and balun at different times 't'.

1. **Assumptions and Approximations**

i. Modelling the bench measurement apparatus as a thin rod

The measurement apparatus is considered to be a thin rod upon which Fourier's One dimensional heat transfer equation can be applied. The temperature distribution is only considered in one dimension (over the rod's length) in this model. No consideration is given to the cross sectional area of the rod. This can be done if the constant of thermal permissivity (m^2/s) for the material is used which takes into account the corresponding increase in thermal mass due to an increased cross sectional area.

ii. Fixed End temperatures

Each end is of the rod is held at a fixed temperature. This is absolutely true only at the chip resistor that is heated or cooled to a fixed temperature. The bar however is made sufficiently long (1m) so that the other end (fixed at room temperature) is kept a sufficient distance from the point at which the LNA is located (approx 0.25m from the chip resistor) to prevent it from affecting the temperature at this point. Looking at the final plot of the temperature distribution over time it can be seen that the rod is at a constant 298K for the times shown over a considerable distance from the 1m fixed end temperature point. This assumption has increased credibility when the thermal mass of the apparatus (connecting cables and power meter) is

considered. We can safely assume therefore that from about 0.4m and greater the temperature is a constant 298K and the fixed end temperature assumption can be applied to both ends.

iii. The rod is laterally insulated

The model takes no account of heat radiation or convection from the rod to the surrounding environment. As we are concerned about minimizing heat transfer to the LNA we are interested in a conservative estimate of the LNA temperature. Because the bench measurement apparatus is originally at 298K ambient temperature, the model will give us a conservative or worst case estimate. Heat transfer to the LNA is therefore predicted to be even less than that indicated by the model.

iv. The thermal permissivity for the whole apparatus is taken as that of copper.

Although the apparatus is constructed from both aluminium and copper as well as other materials, the thermal permissivity of the entire structure is taken as that of copper. This is because it has the greatest permissivity of all the materials used in the balun/taper. Because we are requiring a conservative estimate this will be a satisfactory assumption.

2. Variables used in the model

u_L = 77K – temperature of the chip resistor noise source. 77K is the most distant temperature from the ambient that will be used in the experiment and will therefore have the greatest effect on heat conduction in the apparatus

u_R = 298K – Other end temperature (ambient)

u_0 = 298K – initial temperature of the apparatus (ambient)

L = 1m – length of the rod

$\alpha^2 = 0.000117\, m^2 / s$ – thermal permissivity of copper

3. The Model

After derivation, the heat distribution along x at different times t is given by:

$$HeatDistribution(x,t) = \sum_n C_n \sin\left(\frac{n\pi x}{L}\right) e^{\frac{-\alpha^2 n^2 \pi^2 t}{L^2}} + \left(\frac{u_R - u_L}{L}\right) x + u_L$$

where: …….(12)

$$C_n = 2\frac{(u_L - u_0)}{n\pi}\left[(-1)^n - 1\right] + 2\frac{(u_R - u_L)}{n\pi}(-1)^n$$

Substituting in the variables and constants and evaluating for the times t = 20, 40, 60 and 80 seconds and plotting over the length x results in the solution given in figure 9. The heat distribution at 20s is the dark blue line and at 40s it is green etc. The plot has been produced with the aid of MATLAB. The code is in appendix 3 and is based on the code provided in [8]. It can be seen from the plot that after 20s (a time that is considered adequate for a noise figure measurement) the temperature at the LNA (x = 0.30m) has changed by less than one degree. It can be concluded, therefore, that a stainless steel thermal barrier is not necessary in the construction of the taper.

Figure 9.

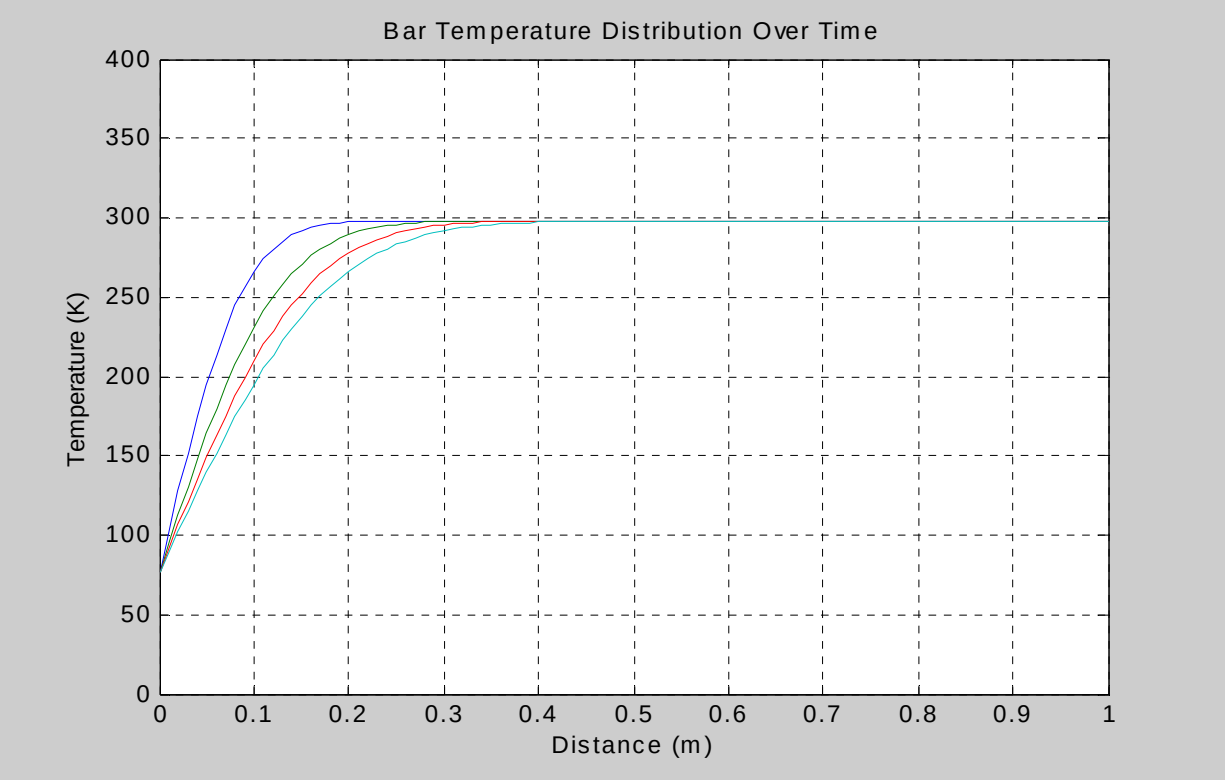

Bracket and Clamp

A simple bracket and clamp was constructed from acrylic as a means for providing mechanical rigidity between the balun and PCB taper. This protects the system from breakage and also ensures repeatable results when measurements are made. Care was taken to avoid having the acrylic in close proximity to conductors where the characteristic impedance would be significantly altered or where the high loss tangent of the acrylic material might increase the system loss. Having any acrylic material in close proximity to the conductors of the PCB taper would significantly effect the loss. A gap is therefore provided in the bracket at the PCB connection point as shown in the figure 11.

Figure 10. – The completed balun/taper

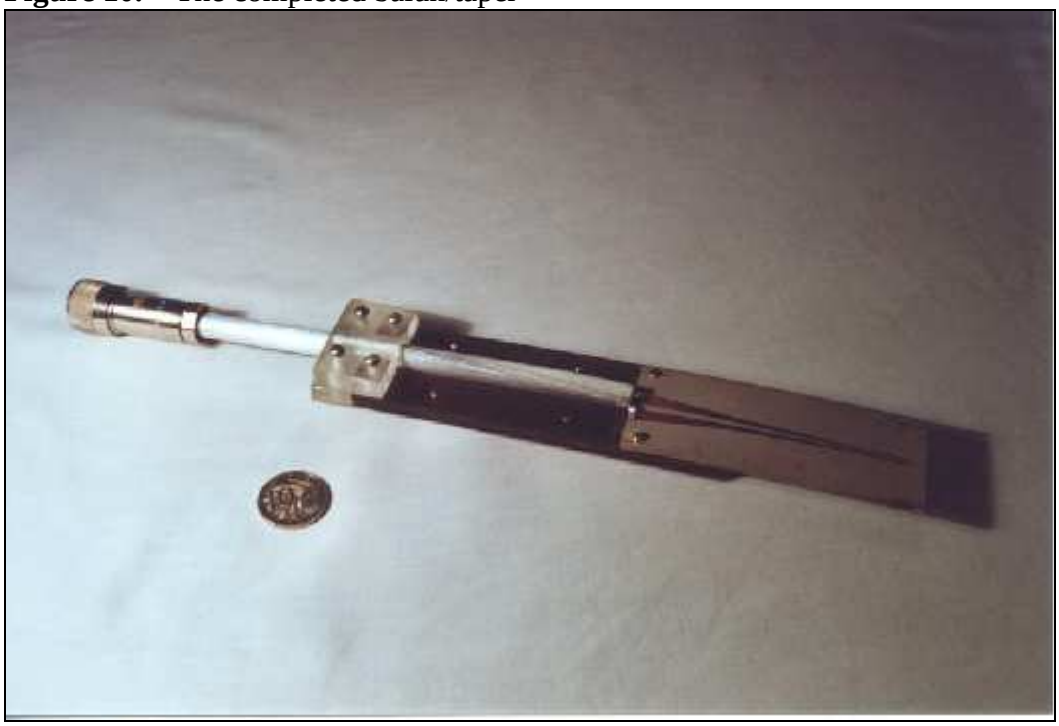

Figure 11. – The underside of the balun/taper. The shape of the bracket can be seen. Notice the gap at the point where the balun connects to the PCB.

Performance Results

A number of tests were performed on the balun/taper. These included:

1. Return loss of balun/taper with bracket. Terminated with a short circuit.
2. Return loss of balun/taper without bracket. Terminated with a short circuit.
3. Return loss of balun/taper with bracket. Terminated with 180Ω.
4. Return loss of balun/taper without bracket. Terminated with 180Ω.

For the short circuit terminations, a solder bridge was formed at the end of the PCB taper. For the 180Ω termination, a 180Ω chip resistor was soldered to the end of the PCB taper.
Measurements were performed using an RF bridge and reflectometer. A diagram of the setup is shown in figure 12.

Figure 12

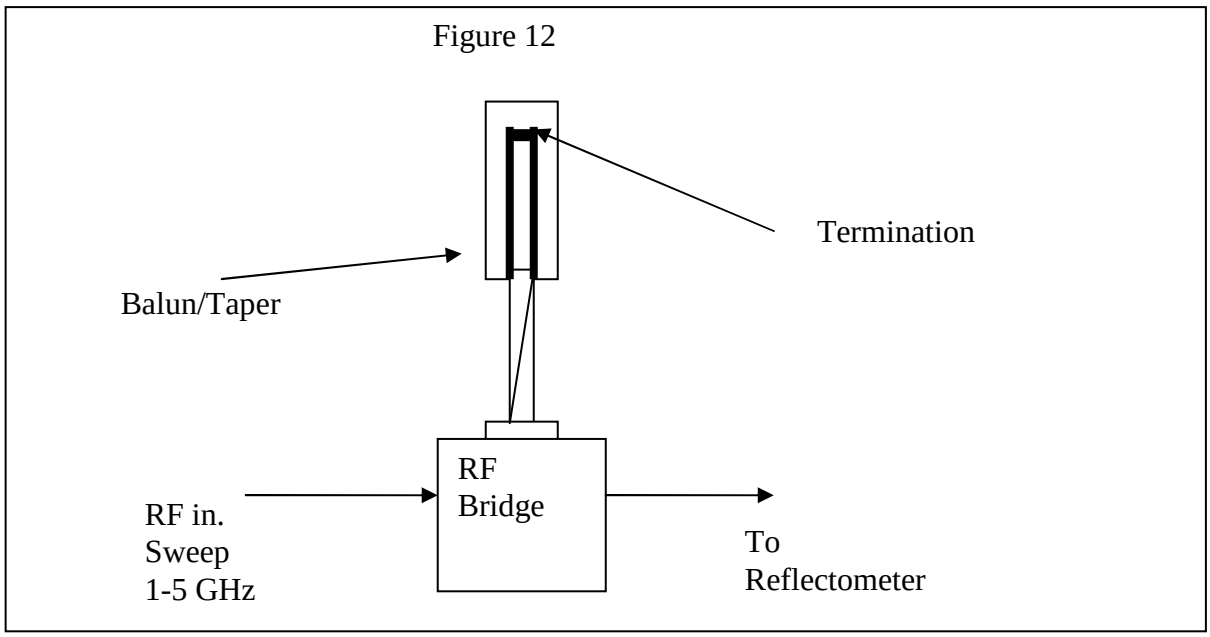

The results for tests 1 and 2 are shown in figure 13. Results for Test 1 are indicated by the blue line and results for Test 2 are indicated by the red line. From this, an indication of the magnitude of loss in the balun/taper can be obtained. Because the system is terminated in a short circuit, all power should be reflected and ideally the reflectometer should register a 0dB return loss. Because losses have occurred as the fields travel towards the termination and back towards the load, the reflectometer registers the amount of loss over the return trip of the signal. In theory, the loss of the balun/taper is half the loss registered by the reflectometer. In practice however, there have been some losses due to radiation and a slight loss of power due to some current flowing down the outside of the coax. Looking at the figure 13 below it can be seen that the presence of the bracket did not significantly affect the loss of the system. The loss is estimated at about 0.2dB.

Figure 13.

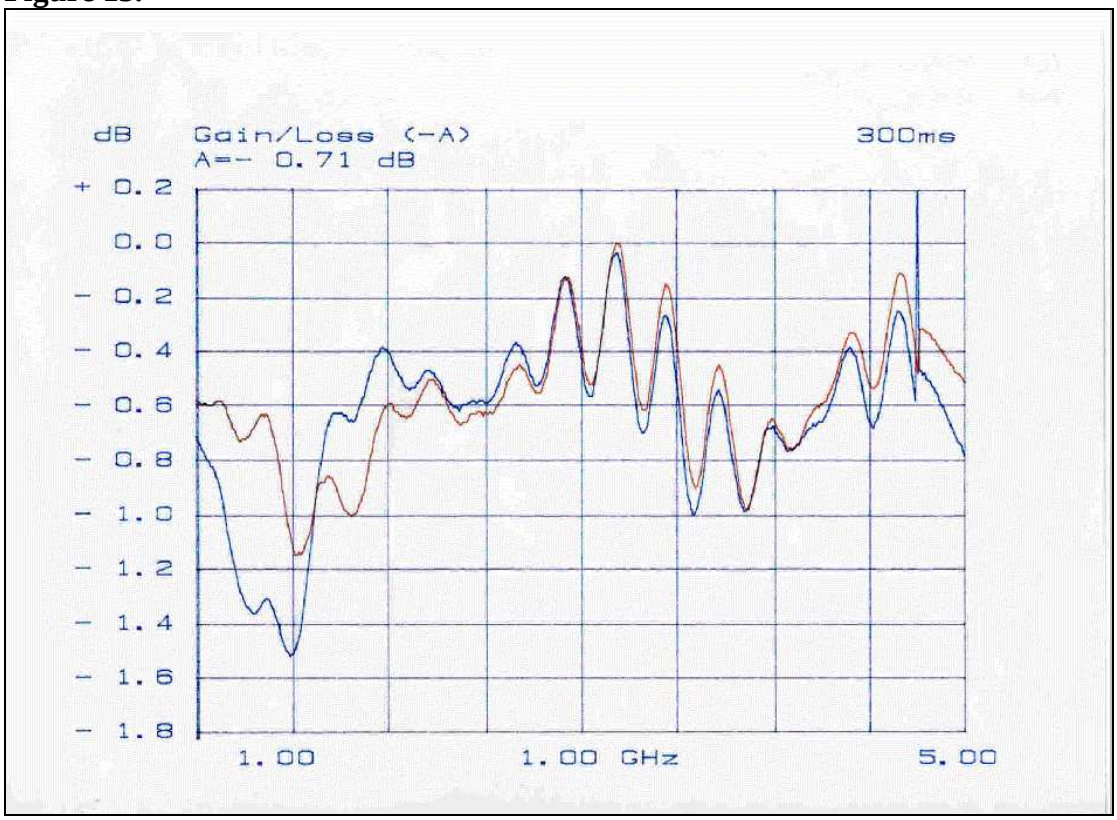

The results for tests 3 and 4 are shown in figure 14. The results for Test 3 are indicated by the blue line and the results for Test 4 are indicated by the red line. The return loss appears to be around –14 dB over the frequency range, corresponding to a voltage reflection coefficient of 20% and an SWR of 1.5.

Figure 14.

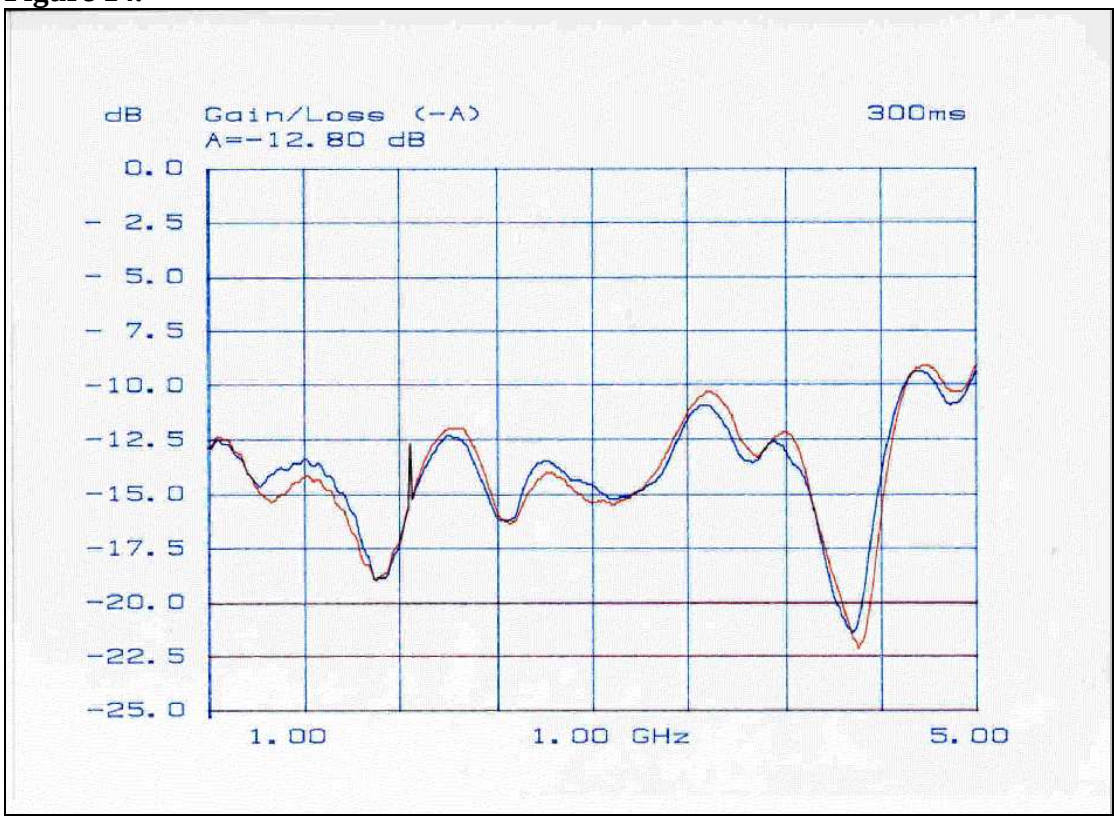

The Klopfenstein Taper used in the system was designed so that the voltage reflection coefficient would not exceed 2%, however, there are a number of reasons why this target has not been reached.

i. The transition from the coaxial balun to the PCB taper results in an abrupt change in the geometry of both the conductors and the dielectric. Reflections would occur at this point

ii. The taper was designed to terminate in 200Ω, however, 180Ω is the closest value available. Even if the taper was perfect, the mismatch caused by this 180Ω resistor on its own would result in a 5.2% reflection coefficient which already exceeds the 2.1% specified in the taper design.

iii. The balun was constructed from hand tools and accurate realisation of the Klopfenstein taper was difficult to obtain. It is predicted that the etching process would provide a more accurate representation of the Klopfenstein Taper.

iv. It is thought that the track widths of the PCB taper are slightly in error near the point where the coaxial balun connects at points 1, 2, and 3 (see figure7). It is believed that the simulation software was not allowed to perform the adequate number of iterations required for the solution to converge completely in this section of the taper. This, however, may not be detrimental to the system performance since the track widths are narrower than that required for the specified characteristic impedance at these points. This may provide some compensation for the abrupt change in geometry at the connection point between the balun and taper by reducing the capacitance at this point.

Performance Evaluation

In general the balun/taper has performed well. It exhibits low loss and the return loss of approximately –14dB is a relatively good result. The pleasing thing about these results is the robustness of the design. That is, the balun was constructed from fairly rudimentary techniques not associated with high precision, the chip resistor does not provide the ideal match and there

is the presence of the abrupt transition. Despite all this the performance is good. This indicates that performance can be easily improved if more precise construction methods are used.

Making the Noise Temperature Measurements

Theory behind noise measurement and errors

To determine the noise temperature of a certain device it is necessary to take at least two measurements of noise power at the output of the device under test with the noise source at two different temperatures. Making the measurements requires a setup similar to that shown in Figure 15.

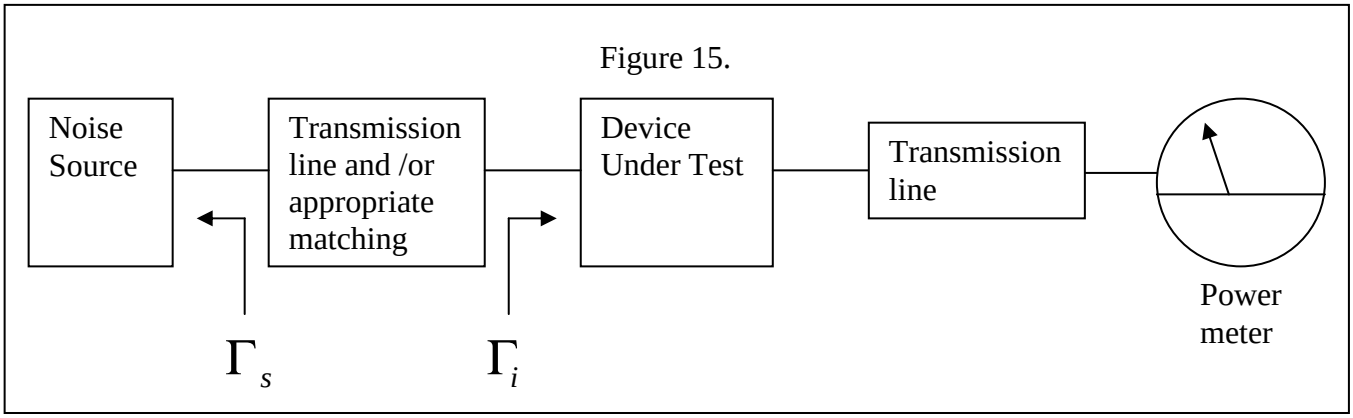

Figure 15.

The method used to determine the noise temperature is based on the Y factor method [9]. A power measurement is taken with the noise source at ambient temperature and this result is recorded. The noise source resistor is then cooled to liquid nitrogen boiling point temperature of 77K and another power measurement is taken and recorded. The results are then plotted with their corresponding temperatures on a graph similar to that shown in figure 16.

Figure 16.

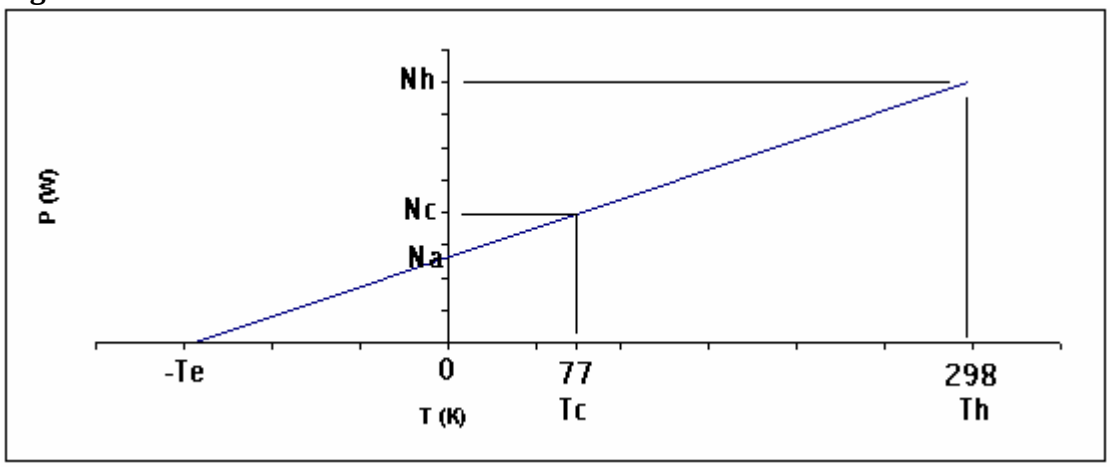

It can be seen from the graph that the intercept of the extrapolated line with the temperature axis gives the negative noise temperature T_e of the device under test [9]. The extra noise added by the device under test is denoted N_a. It can be seen from the graph that it is only necessary to determine a ratio of N_h to N_c. It is not necessary to obtain the magnitude of each. As long as the measured powers are measured in correct proportion to each other, the intercept at $-T_e$ will remain the same.

Provided that the noise measurements are accurate, and system losses and reflections remain constant at different noise source temperatures, the value for T_e obtained will be accurate.

Unfortunately this is not the case when a practical noise temperature measurement is performed. The requirement to measure low noise figures below 1 dB makes high measurement accuracy difficult to obtain.

If the various reflection coefficients remained constant over measurements at different temperatures, the effects of reflections in the measurements of N_h and N_c would be the same. Since this would not alter the proportion between the two measurements the intercept at the temperature axis would provide an accurate indication of the noise temperature. This is because the determination of T_e requires only ratiometric power measurements.

The problems associated with reflections become great when the system's reflections change as the noise source is heated and cooled. Reflections are the greatest source of error in determining T_e. Consider figure 15 in which the reflection coefficient looking into the noise source is Γ_s and the reflection coefficient looking into the input of the Device Under Test (DUT) is Γ_i. From [10], the power from the noise source dissipated by the LNA's input terminals is given by:

$$P_d = |b_s|^2 \frac{1-|\Gamma_i|^2}{|1-\Gamma_s\Gamma_i|^2} \quad \text{…….(13)}$$

and the power incident on the input terminals of the LNA is given by:

$$P_i = |b_s|^2 \frac{1}{|1-\Gamma_s\Gamma_i|^2} \quad \text{…….(14)}$$

where $|b_s|^2$ is the available power of the noise source.

As defined in [11], the available noise power at the input to the LNA is the noise power that would be absorbed by the LNA if it were perfectly matched. In the perfectly matched case when Γ_i =0, equation 14 becomes $P_i = |b_s|^2$. It is the incident power P_i that is amplified by the LNA to obtain the power P_o that appears at the output terminals of the LNA.

Therefore

$$P_o = GP_i \quad \text{…….(15)}$$

Where G is the gain of the LNA.

And $$P_o = G|b_s|^2 \frac{1}{|1-\Gamma_s\Gamma_i|^2}. \quad \text{…….(16)}$$

Where $G|b_s|^2$ is the available power at the output terminals of the LNA.

Rearrange equation 16 to obtain:

$$G|b_s|^2 = P_o|1-\Gamma_s\Gamma_i|^2. \quad \text{…….(17)}$$

Knowing the amplitude and phase of Γ_s and Γ_i enables the determination of $G|b_s|^2$ from P_o. Unfortunately, only the magnitude of Γ_s and Γ_i can be easily measured or estimated.

With only the magnitude of Γ_s and Γ_i it is only possible to determine the value of $G|b_s|^2$ within some limits.

These limits are:

$$G|b_s|^2{}_{MAX} = P_o(1+|\Gamma_s||\Gamma_i|)^2$$

and

$$G|b_s|^2{}_{MIN} = P_o(1-|\Gamma_s||\Gamma_i|)^2. \quad \text{…….(18)}$$

Therefore:

$$P_o\left(1-|\Gamma_s||\Gamma_i|\right)^2 \le G|b_s|^2 \le P_o\left(1+|\Gamma_s||\Gamma_i|\right)^2 \qquad \text{…….(19)}$$

Knowing these limits gives the level of uncertainty of the available noise power at the terminals of the LNA when P_o is known. It is assumed here that the power meter is well matched to the transmission line that connects between itself and the LNA's output terminals so that any re-reflections between the LNA and the power meter are kept negligible. To ensure that re-reflections do not occur it is recommended that a suitable attenuator be placed at the power meter's input terminals so that any possible reflections from the power meter will be absorbed. For this reason, uncertainty due to mismatch will only be considered on the input side of the LNA.

This leaves another uncertainty to consider. The uncertainty associated with the power reading obtained from the power meter. This means that the power available at the LNA output terminals P_o may also lie within some limits.

i.e.

$$P_{o-LowerLimit} \le P_o \le P_{o-UpperLimit}$$

$$P_{MEASURED}\left(1-P_E\%\right) \le P_o \le P_{MEASURED}\left(1+P_E\%\right) \qquad \text{…….(20)}$$

Where $P_{MEASURED}$ is the power measurement taken from the power meter, and $P_E\%$ is the percentage error associated with the power meter.

Combining (19) with (20) and letting $N = G|b_s|^2$,

$$P_{MEASURED}\left(1-P_E\%\right)\left(1-|\Gamma_s||\Gamma_i|\right)^2 \le N \le P_{MEASURED}\left(1+P_E\%\right)\left(1+|\Gamma_s||\Gamma_i|\right)^2. \qquad \text{…….(21)}$$

Where N is the noise power that is plotted on the graph in figure 16 for the hot and cold measurements N_c and N_h.

The upper and lower errors due re-reflections (not including power meter error) are given in percentages in the table 5 below for various combinations of $|\Gamma_s|$ and $|\Gamma_i|$. Calculated values are from (21).

Table 5a - Upper percentage error due to re-reflection

$\lvert\Gamma_i\rvert$ \ $\lvert\Gamma_s\rvert$	**0.01**	**0.05**	**0.1**	**0.2**	**0.3**
0.1	0.2	1.0	2.0	4.0	6.1
0.2	0.4	2.0	4.0	8.2	12.4
0.3	0.6	3.0	6.1	12.4	18.8
0.4	0.8	4.0	8.2	16.6	25.4
0.5	1.0	5.1	10.3	21.0	32.3
0.6	1.2	6.1	12.4	25.4	39.2
0.7	1.4	7.1	14.5	30.0	46.4
0.8	1.6	8.2	16.6	34.6	53.8
0.9	1.8	9.2	18.8	39.2	61.3

Table 5b - Lower percentage error due to re-reflection

$\lvert\Gamma_i\rvert$ \ $\lvert\Gamma_s\rvert$	**0.01**	**0.05**	**0.1**	**0.2**	**0.3**
0.1	-0.2	-1.0	-2.0	-4.0	-5.9
0.2	-0.4	-2.0	-4.0	-7.8	-11.6
0.3	-0.6	-3.0	-5.9	-11.6	-17.2
0.4	-0.8	-4.0	-7.8	-15.4	-22.6
0.5	-1.0	-4.9	-9.8	-19.0	-27.8
0.6	-1.2	-5.9	-11.6	-22.6	-32.8
0.7	-1.4	-6.9	-13.5	-26.0	-37.6
0.8	-1.6	-7.8	-15.4	-29.4	-42.2
0.9	-1.8	-8.8	-17.2	-32.8	-46.7

It can be seen from the above two tables that even if the Device Under Test has a reflection coefficient that is high in magnitude, the error can be kept low if the reflection coefficient of the noise source is kept low.

From the graph it is obvious that the noise temperature T_e can be calculated from

$$T_e = \frac{N_c(T_h - T_c)}{N_h - N_c} - T_c . \qquad \text{…….(22)}$$

The approximate errors associated with the determined value of T_e in terms of the error in the cold measurement and the hot measurement are given by

$$Error = (E_c + E_h)\left(1 + \frac{T_c + T_e}{T_h - T_c}\right)\left(\frac{T_c + T_e}{T_e}\right). \qquad \text{…….(23)}$$

Where E_c is the upper percentage error limit associated with the cold measurement, and E_h is the upper percentage limit associated with the hot measurement.

E_c and E_h can be approximated as the sum of the error due to re-reflection and the power meter error.

An indication of how these errors and the expected value of T_e affects the overall error in the determination of T_e is shown in the table 6.

Table 6.

Te=10K
Approximate percentage error of Te

	Ec						
Eh	**0.5**	**1**	**2**	**4**	**8**	**16**	**32**
0.5	12	18	30	55	103	200	394
1	18	24	36	61	109	206	400
2	30	36	48	73	121	218	412
4	55	61	73	97	145	242	436
8	103	109	121	145	194	291	485
16	200	206	218	242	291	388	582
32	394	400	412	436	485	582	776

Te=20K
Approximate percentage error of Te

	Ec						
Eh	**0.5**	**1**	**2**	**4**	**8**	**16**	**32**
0.5	7	10	17	31	59	115	227
1	10	14	21	35	63	119	230
2	17	21	28	42	70	126	237
4	31	35	42	56	84	140	251
8	59	63	70	84	112	167	279
16	115	119	126	140	167	223	335
32	227	230	237	251	279	335	447

Te=30K
Approximate percentage error of Te

	Ec						
Eh	**0.5**	**1**	**2**	**4**	**8**	**16**	**32**
0.5	5	8	13	24	45	87	172
1	8	11	16	26	48	90	175
2	13	16	21	32	53	95	180
4	24	26	32	42	64	106	191
8	45	48	53	64	85	127	212
16	87	90	95	106	127	169	254
32	172	175	180	191	212	254	339

Te=50K
Approximate percentage error of Te

	Ec						
Eh	**0.5**	**1**	**2**	**4**	**8**	**16**	**32**
0.5	4	6	10	18	34	66	130
1	6	8	12	20	36	68	132
2	10	12	16	24	40	72	136
4	18	20	24	32	48	80	144
8	34	36	40	48	64	96	160
16	66	68	72	80	96	128	192
32	130	132	136	144	160	192	256

Te=70K
Approximate percentage error of Te

	Ec						
Eh	**0.5**	**1**	**2**	**4**	**8**	**16**	**32**
0.5	3	5	9	16	30	58	114
1	5	7	10	17	31	59	115
2	9	10	14	21	35	63	119
4	16	17	21	28	42	70	126
8	30	31	35	42	56	84	140
16	58	59	63	70	84	112	168
32	114	115	119	126	140	168	224

It can be seen from table 6 that even a small error in the hot and cold measurement such as 4% can compound into a large error in the final determination of T_e.

Applying noise temperature measurement to the LNA and Balun/transformer

Case 1. Using balun/transformer to measure noise temperature of LNA.

In this case the connections shown in figure 17 are required

Figure 17

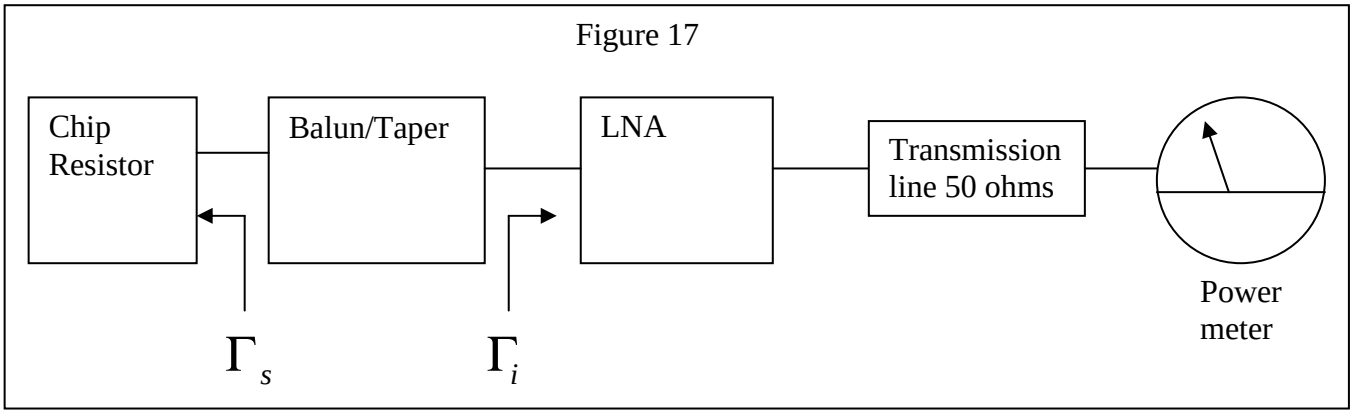

From the performance measurements of the balun/taper, the magnitude of Γ_s can be estimated at about 0.2 at 298K (assuming that the magnitude of the reflection coefficient of the balun/taper is equal on its input and output side). Γ_s is not known for 77K but for the purposes of this example it will be assumed to be 0.2 also. The magnitude of Γ_i depends on the value of S_{11} for the LNA and this could be as high as 0.9. To examine what the effect of reflections in this arrangement would have on the errors, consider the values of $|\Gamma_s|$ and $|\Gamma_i|$ to be 0.2 and 0.6 respectively for both the hot and cold measurements.
Looking at table 5a and assuming that the power meter error is small, it can be seen that power measurements made for N_c and N_h could be in error by approximately 25% (upper limit). Assuming the noise temperature to be around 50K and looking then at table 6, it can be sent that this error results in a final error for T_e somewhere between +/-128% and +/256%. This is clearly not a good indication of the noise temperature and it is therefore not recommended to use the balun/taper to measure the noise temperature of the LNA in this way.

Case 2. Using a microstrip line to measure noise temperature of LNA.

Due to the large reflection coefficient Γ_s associated with the balun/taper, the noise temperature of the LNA is virtually impossible to measure with sufficient accuracy in the previous case. It is therefore recommended to employ a low loss microstrip line of constant characteristic impedance between the noise source resistor and the LNA. This is similar to the approach adopted in [12]. The microstrip line can be easily manufactured and will provide for a much better match for the noise source resistor. The resistance of the chip resistor and the microstrip characteristic impedance will be equal to that required by the non-standard input impedance of the LNA.

Figure 18.

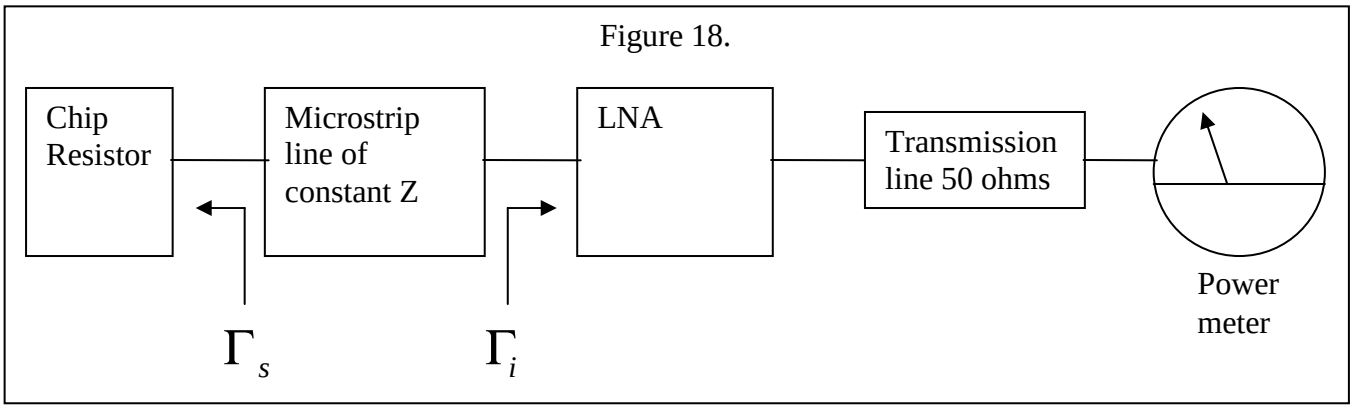

Consider now that the resistor is matched to the microstrip line with a reflection coefficient of only 0.01 at room temperature. Taking $|\Gamma_s|$ as 0.01 for the hot measurement and 0.05 for the cold measurement and $|\Gamma_i|$ as 0.6 and looking in table 5, it can be seen that the upper error limit for the hot measurement is about 1% and the upper error limit for the cold measurement is about 6%. Assuming that the expected noise temperature of the LNA is about 50K, the expected error associated with the determination of T_e is somewhere between +/-20% and +/-36% (from table 6). This is a vast improvement to the case in which the balun and taper were used to connect the noise source to the LNA. It can be seen from this example how critical the correct matching of the noise source to the line is to achieving a value of T_e with minimum error.

Case 3. Measuring Noise Temperature of the Balun/taper and LNA together

The Noise Temperature of the balun/taper and the LNA combined together as one "Device Under Test" can be determined with better accuracy than in the first case where the balun/taper is used in an attempt to determine the noise temperature of the LNA alone.

Figure 19.

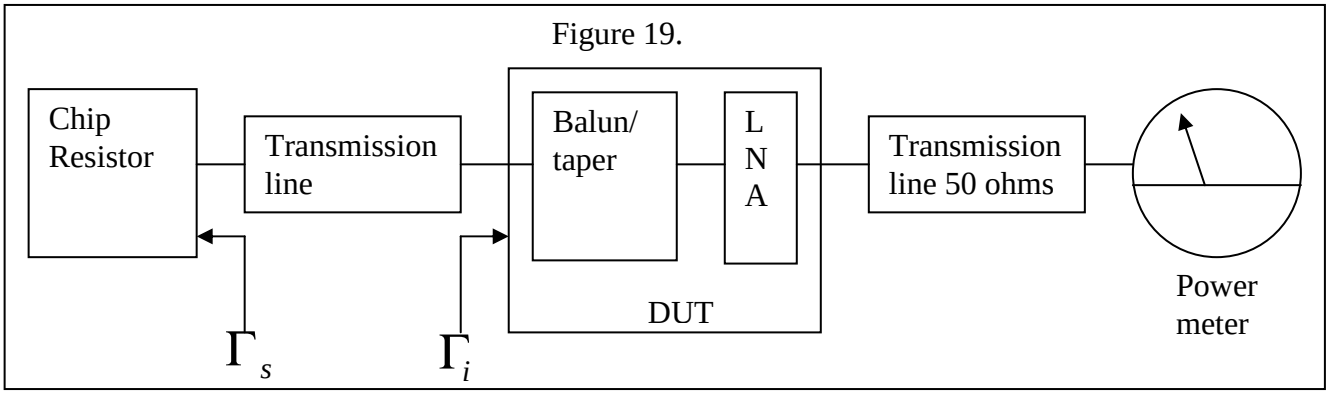

It can be seen from the above diagram that it is now required to determine $|\Gamma_i|$ for the "Device Under Test" which consists of both the balun/taper and the LNA. This is difficult to determine, but an upper limit for this can be determined if the input reflection coefficient of the LNA and the Balun/Taper is known. Refer to figure 20.

Figure 20.

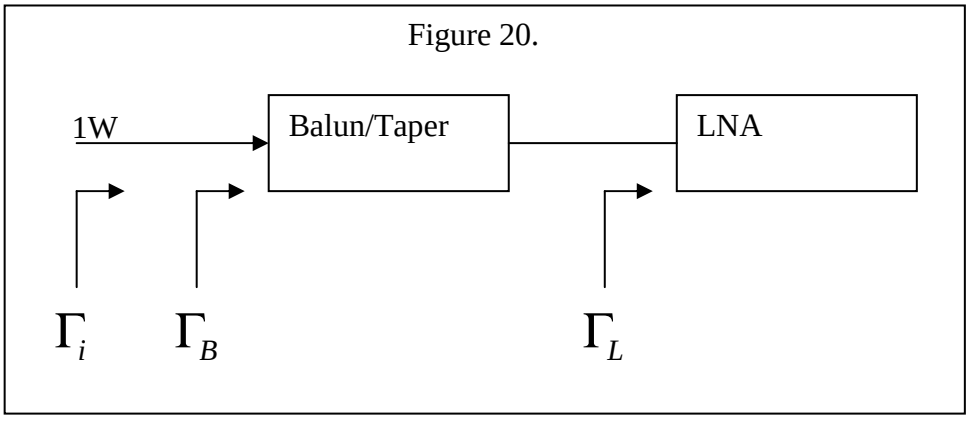

Γ_L can easily be determined from S_{11} of the LNA. As an example $|\Gamma_L|$ is given the value 0.6. Assuming that the magnitude of the reflection coefficient of the 200Ω side of the balun/taper is equal to its 50Ω side (which may not necessarily be the case) $|\Gamma_B|$ is given the value of 0.2 that was measured on the 50Ω side.

Consider 1W of power being incident at the point shown. Due to $|\Gamma_B|$ the power incident on the input terminals of the LNA is equal to $1-|\Gamma_B|^2 = 1-0.2^2 = 0.96 Watts$. The power that never reaches the LNA is $|\Gamma_B|^2 = 0.04 Watts$ and this is reflected back towards the source. The magnitude of the reflection coefficient at the LNA terminals is $|\Gamma_L|$ and of the 0.96Watts incident, $0.96\times|\Gamma_L|^2 = 0.96\times 0.6^2 = 0.3456 Watts$ is reflected back to the source. Adding up the reflected power (0.04+0.3456=0.3856W), the reflection coefficient of the entire "Device Under Test" can be determined by finding the square root of this reflected power to determine the reflected voltage. As a result, $|\Gamma_i|$ becomes 0.62.

In summary, $|\Gamma_i|$ can be calculated using:

$$|\Gamma_i| = \sqrt{|\Gamma_B|^2 + \left(1-|\Gamma_B|^2\right)|\Gamma_L|^2} \qquad \text{…….(23)}$$

This value for $|\Gamma_i|$ is the upper limit for the reflection coefficient of the "Device Under Test". An exact value of $|\Gamma_i|$ cannot be determined easily. This value was calculated based on the assumption that the reflection coefficient of the balun/taper is the same at both ends. If a balun/taper with a non standard coaxial connection other than 50Ω is used $|\Gamma_B|$ will be even more difficult to estimate because the device cannot be connected to standard test equipment. In this case one will need to make a conservative estimate of $|\Gamma_B|$ taking into account its effect on the value of $|\Gamma_i|$. In order to make this estimate, one should look at how various values of $|\Gamma_B|$ affect the value of $|\Gamma_i|$. Consider the table below.

Table 7. – Determining $|\Gamma_i|$

$\|\Gamma_B\|$	Return Loss (dB)	$\|\Gamma_L\|$ 0.1	0.2	0.3	0.4	0.5	0.6	0.7	0.8	0.9
0.1	-20.0	0.14	0.22	0.31	0.41	0.51	0.61	0.70	0.80	0.90
0.2	-14.0	0.22	0.28	0.36	0.44	0.53	0.62	0.71	0.81	0.90
0.3	-10.5	0.31	0.36	0.41	0.49	0.56	0.65	0.73	0.82	0.91
0.4	-8.0	0.41	0.44	0.49	0.54	0.61	0.68	0.76	0.84	0.92
0.5	-6.0	0.51	0.53	0.56	0.61	0.66	0.72	0.79	0.85	0.93
0.6	-4.4	0.61	0.62	0.65	0.68	0.72	0.77	0.82	0.88	0.94
0.7	-3.1	0.70	0.71	0.73	0.76	0.79	0.82	0.86	0.90	0.95
0.8	-1.9	0.80	0.81	0.82	0.84	0.85	0.88	0.90	0.93	0.97
0.9	-0.9	0.90	0.90	0.91	0.92	0.93	0.94	0.95	0.97	0.98

For example the reflection coefficient of the LNA is known to be 0.6 but the reflection coefficient of the balun at the balanced end is uncertain. What may be known, however, is that the reflection coefficient is better than 0.4 corresponding to a return loss better than 8 dB. Knowing this we can place an upper bound on $|\Gamma_i|$ at 0.68.

Knowing a value for $|\Gamma_i|$ it is now necessary that the noise source resistor is well matched to the unbalanced transmission line between the resistor and balun/taper. This line is necessary to provide some thermal isolation between the balun/taper and noise source. As in the previous cases the error in N_c and N_h can now be determined and finally the error in T_e also. As in case 2, it is very

important to ensure that the noise source resistor is well matched to the connecting transmission line so that a minimum error can be obtained.

General Procedure for determining noise temperature

The following outlines a procedure for determining the noise temperature of a device under test. An example is given simultaneously for the situation given in Case 3 in which the overall noise temperature of the balun taper and LNA is determined. The numerical values given in the example do not apply to the balun/taper that has been constructed and are purely hypothetical.

1. **Determine $|\Gamma_i|$ from LNA design, or where appropriate find the upper limit of $|\Gamma_i|$ from the procedure outlined in Case 3.**
   It is known from the LNA's S_{11} that the magnitude of its reflection coefficient is 0.6. The reflection coefficient of the balun/taper at the balanced terminal is unknown, however, the return loss is known to be at least better than –10dB. Looking at table 7 to see where the –10dB return loss row intersects with the $\Gamma_L = 0.6$ column, it can be seen that the upper limit of the DUT reflection coefficient $|\Gamma_i|$ is equal to 0.65.

2. **Determine $|\Gamma_s|$ or upper limit of $|\Gamma_s|$ for noise source at both hot temperature and cold temperature. This can be determined by the following method:**
   If the characteristic impedance of the transmission line Z_L at the point of attachment of the resistor is known, and the DC resistance of the resistor is measured at both hot and cold temperatures, $|\Gamma_s|$ at both these temperatures can be easily determined from:
   $$|\Gamma_s| = \left|\frac{R - Z_L}{R + Z_L}\right| \qquad \text{…….(24)}$$
   It is known for example, that the noise source chip resistor is attached to a balanced PCB twin line of which the characteristic impedance is accurately known at 180Ω. The probes of a DC ohmmeter are applied to the unbalanced terminal and the resistance of the chip resistor at room temperature (e.g. 290K) is measured at 184Ω. The chip resistor is then immersed in liquid nitrogen and after the vigorous boiling has ceased another DC resistance measurement is made. At this time the resistance is 163Ω. From these two measurements $|\Gamma_s|$ can be determined from the equation above at both 290K(hot) and 77K(cold) temperatures. In this case, $|\Gamma_{s(hot)}| = 0.01$ and $|\Gamma_{s(cold)}| = 0.05$.

3. **Check that the noise temperature to be obtained will lie within reasonable error limits. Use tables 5 and 6. Or use equation 23.**
   Looking at table 5 it can be seen that the upper percentage error mismatch limit of the hot measurement is approximately 1.3% and upper percentage error mismatch limit of the cold measurement is approximately 6.6%. The power meter measurement error is 2%. E_c and E_h can be approximated as the sum of the mismatch uncertainty errors and the power meter measurement error. Therefore, E_h =3.3% and E_h =8.6%. Estimating the noise temperature to be somewhere near 50K equation 23 or table 6 can be used to determine the expected error. Looking at table 6 for 50K it can be seen that the expected error will be around 40-48%.

4. **Connect system as in figure 15.**

Since both the balun/taper and the LNA are the device under test, the arrangement in Case 3 will be used. It is necessary to provide some open wire transmission line between the end of the taper and the noise source resistor as shown in figure 19. As in part 2 it is necessary to ensure that the transmission line's characteristic impedance is accurately known. Also the transmission line must be long enough to prevent significant cooling of the balun/taper and LNA (or whatever the DUT may be) when the noise source is cooled.

5. **Make a power measurement with the noise source at room temperature. Use an attenuator at the power meter's input to ensure that any possible re-reflections are minimised. Record the room temperature in Kelvins along with the power measurement N_h.**
   For example, assume that the power measured was 1100mW at T = 290K.

6. **Immerse the chip resistor in Liquid Nitrogen and wait until the vigorous boiling subsides before making another power measurement. Record this measurement N_c with 77K noise source temperature. Do not wait longer than necessary when making this measurement. Observe the heat conduction model to ensure that the Device Under Test is not being significantly cooled.**

   The heat conduction model can apply to any long thin copper structure. It is therefore valid for the connecting transmission line as well as the balun/taper.
   Assume that the power measured was 400mW at T=77K.

7. **Use equation 22 and 23 or use the spreadsheet to obtain the value of T_e and an error. The spreadsheet is simpler to use and provides a more accurate error result and is therefore recommended. An explanation of the spreadsheet calculation is given in appendix 5.**

   In the spreadsheet enter the values 0.05, 0.01, 0.65, and 2 for Gs(cold), Gs(hot), Gi, and Pe% respectively. Enter the cold and hot temperatures of 77K and 290K as well as the corresponding measurements of 400 and 1100mW. Power units are not important as long as they are on a linear scale. The noise temperature is calculated to be approximately 47K with an error of +/-48%.

Conclusion

The design and construction of the required balun/taper has been presented. With only simple construction methods and components the balun and taper achieves good return loss of about –14dB between 1 and 5 GHz. Dielectric and conductor loss combined is less than 0.2dB within the frequency range. It can be seen that good results have been achieved even with the presence of various discontinuities and mismatches. The design is therefore very robust and an improvement in the results could be easily achieved.

If it is required to produce similar baluns it is recommended that the etching process be perfected so that construction is easier. However, building a balun for a non-standard impedance match would not require a piece of commercially available coax. A hollow copper tube would probably be needed instead. This would not be compatible with the etching process described in this paper because the inner surface of the tube would not be protected by dielectric material. One would probably need to resort to sawing or machining in this case.

It has been outlined in this paper that using the balun/taper as a matching device between a chip resistor and LNA would produce noise temperature measurements that have excessive errors. An alternative has been suggested and this requires that a microstrip line be used as the connection between the LNA and noise source. This would simplify the problem of achieving a good match at the noise source. A method has, however, been suggested that would allow the noise temperature measurement of a balun/taper and LNA combination as a single device under test.

Finally, a number of spreadsheet tools have been produced for Klopfenstein Taper design, characteristic impedance of slotted coax, and a spreadsheet that calculates the noise temperature with errors of a device.

What still needs to be done is to provide method by which the heat distribution in the connecting line between the noise source and the DUT can be accurately modelled. From this, a method of calculating the noise contribution of the connecting line can be determined so that a compensation can be made in the final result for noise temperature. If this is not adopted it is essential that this connected line exhibits low loss.

References

1. A. Parfitt, L Milner, "*The Design of Active Receiving Antennas for Broadband Low-Noise Operation*", CSIRO.
2. J. W. Duncan and V. P. Minerva, "*100:1 Bandwidth Balun Transformer*", Proc. IRE, vol. 48, pp. 156-164, February 1960.
3. R. W. Klopfenstein, "*A Transmission Line Taper of Improved Design*", Proc. IRE, vol. 44, pp. 31-35, January 1956.
4. M. A. Grossberg, "*Extremely Rapid Computation of the Klopfenstein Impedance Taper,*" Proc. IEEE, vol. 56, pp 1629-1630, September 1968.
5. J. Carlsson, L Hasselgren, D. Nunez, U. Lundgren, J. Delsing, M. Hoerlin, "*A Systematic Methodology for the Generation of SPICE Models Feasible for EMC Analysis*", SP Swedish National Testing and Research Institute, http://www.sp.se/electronics/RnD/software/eng/fd2d.htm
6. W. Jackson, "*High Frequency Transmission Lines*", Methuen and Co Ltd, London, John Wiley and Sons Inc, 1951.
7. R. A. Chipman, "*Theory and Problems of Transmission Lines*", McGraw-Hill, 1968.
8. J. R. White, "*Mathematical Methods (10/24.539) X. Analytical Solutions of PDEs Example 10.2 – Heat Transfer in a Finite Bar with Fixed End Temperatures*", University of Massachusetts Lowell.
9. T. H. Lee, "*Noise Figure Measurement*", Stanford University, 2002
10. A. Lymer, "*Improving Measurement Accuracy by controlling Mismatch Uncertainty*", Agilent Technologies.
11. H. T Friis, "*Noise Figures of Radio Receivers*", Proc. IRE, pp 419-422, July 1944.
12. J. G. Bij de Vaate, E. E. M. Woestenburg, R. H. Witvers, R. Pantaleoni, "*Decade Wide Bandwidth Integrated Very Low Noise Amplifier*", Netherlands Foundation for Research in Astronomy.

Appendix 1 – Design Drawing of Balun

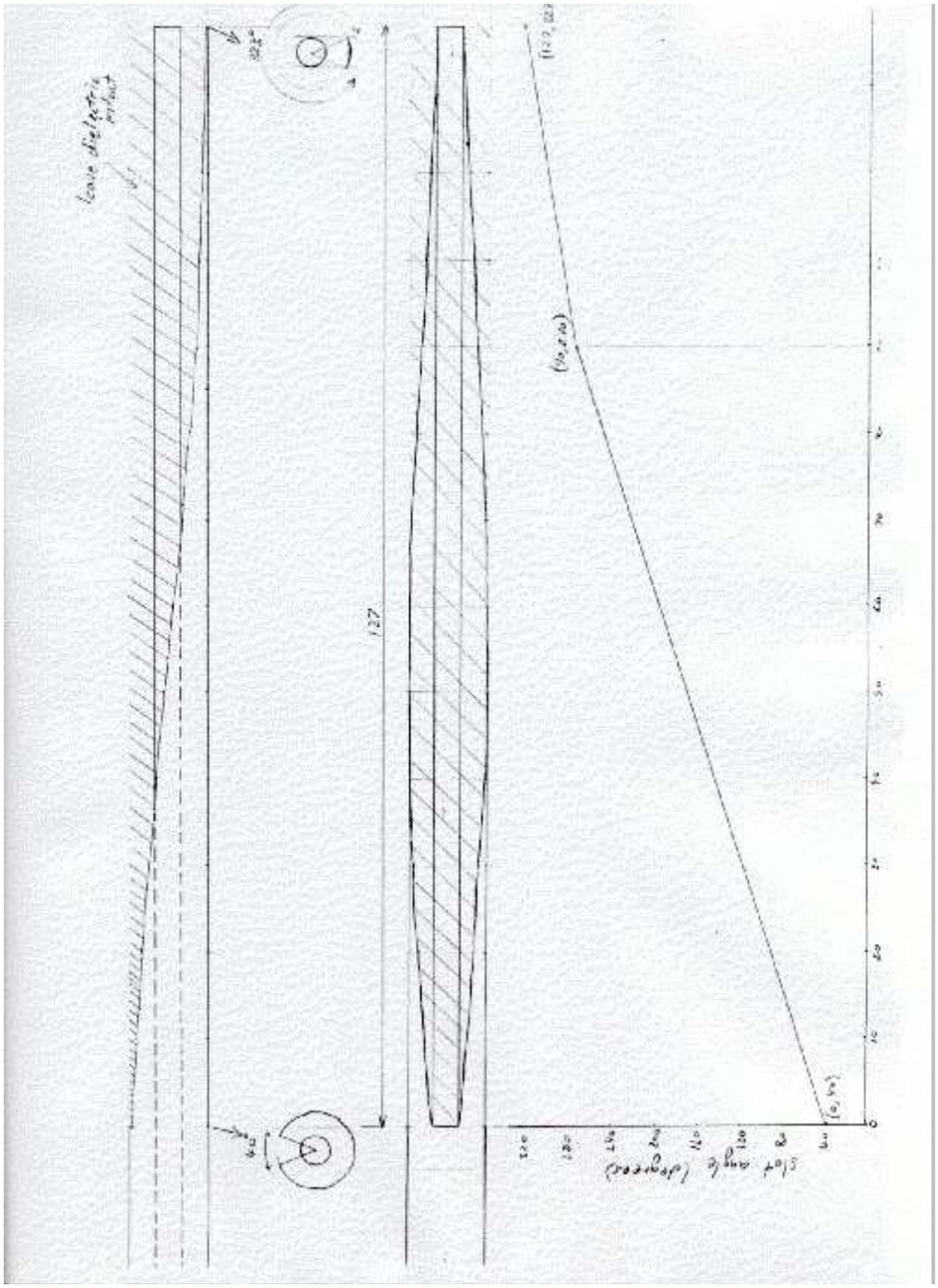

Appendix 2 – Determining the proximity effect on currents in the PCB Taper Line

An approximate value of the proximity factor is calculated using a relatively crude method, however, the results are deemed satisfactory for estimation purposes. To calculate the proximity factor it is necessary to determine the current distribution in the transmission line conductors. The more evenly distributed the currents are within the skin depth of the conductor the lower the proximity factor and the lower the resistive losses. i.e. When currents are evenly distributed around the perimeter of the conductor the proximity factor is at its lowest value of 1.

To determine the current distribution along the conductors the two dimensional cross section of the transmission line is broken up into a series of point sources. In the first iteration the current distribution is considered to be equal along the conductors and each point source is given a current level of 1.These point sources are then used to determine the H field at an equal distance around the perimeter of the conductor. A very crude application of Ampere's law is then performed around each point and the relative current distribution between points is then determined from the relative strengths of the H field. The currents are then normalised with respect to the highest current level and this new current distribution is then used in the next iteration. The iterations are repeated until the current distributions have converged.

Example.
Consider a twin line PCB transmission line with width w=4 and spacing s=3. The line cross section is broken up into points. Each point on a conductor is assigned the current magnitude 1. The directional indicators represent the direction of current flow in the two conductors.

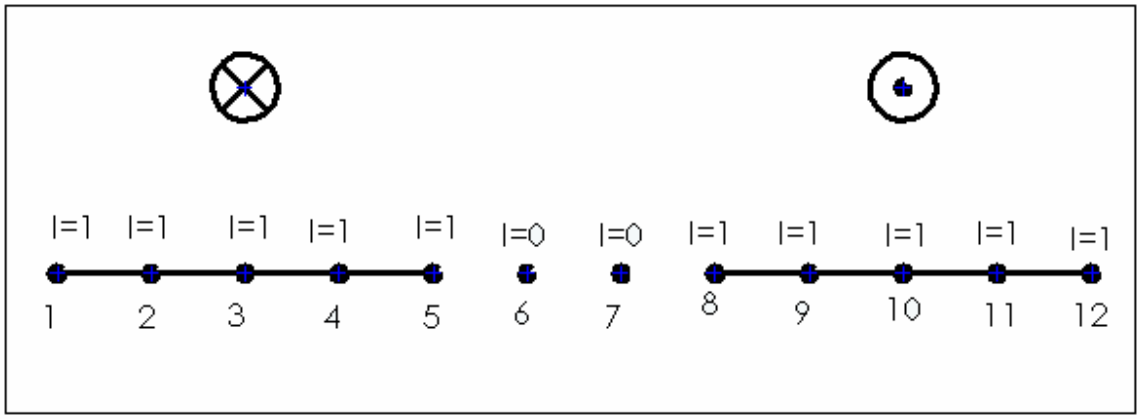

It is then required to find the relative H field strengths in the positions marked in the diagram below:

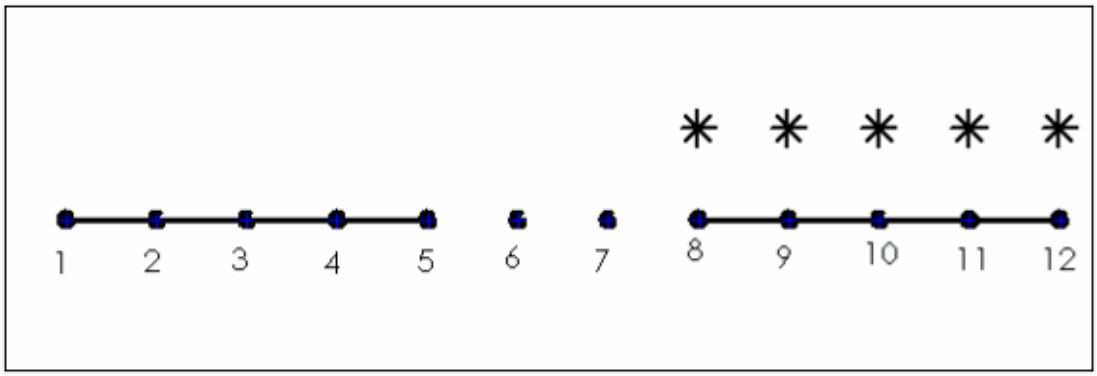

To do this it is necessary to compute the vector sum of each relative contribution from each point on the conductors at the marked positions. To see how the contribution of each point is affected by distance it is necessary to look at Ampere's Law.

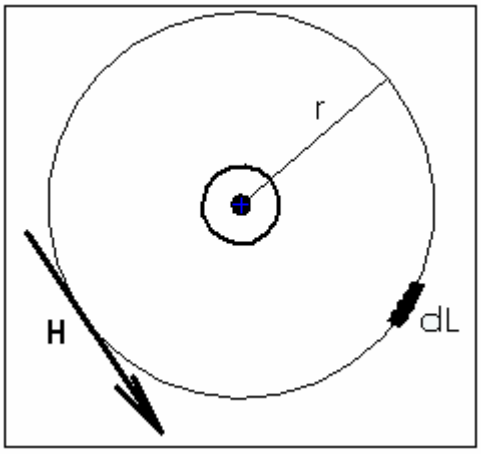

$$I = \oint H \bullet dL \quad \text{(A)}$$

In the case in the diagram, evaluating the line integral around the closed contour of radius r, the expression for current becomes:

$I = H \times 2\pi r$

and

$$H = \frac{I}{2\pi r}$$

which means that the magnetic field is inversely proportional to the distance. In the case of the model the field strength relative to a distance of one element spacing from a point source will be given by:

$$H_{relative} = \frac{1}{r}.$$

To sum the contributions from each point it is necessary to determine the distances between points and to determine the horizontal and vertical components of the magnetic field strength.

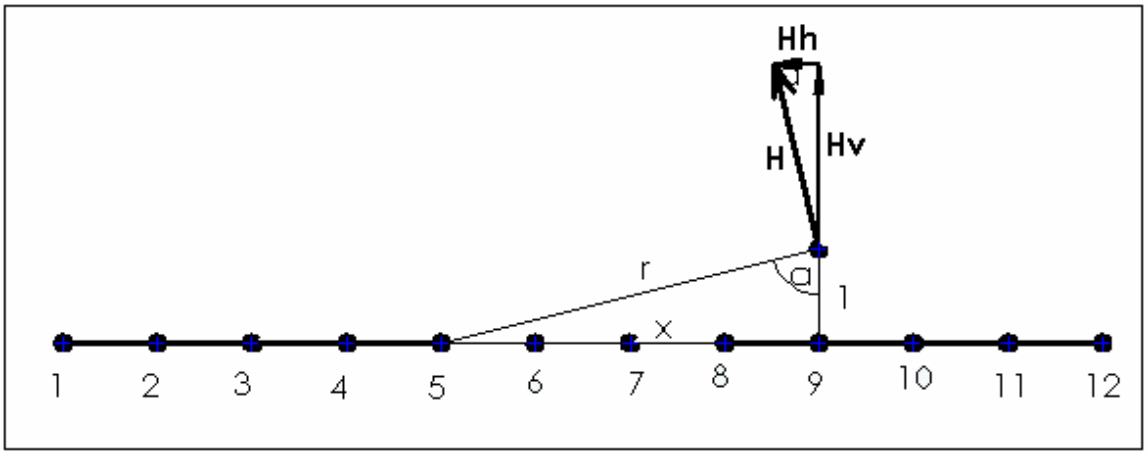

From the above diagram and taking the positive directions to be upward and right:

$a = \tan^{-1} x$,

$$r = \frac{1}{\cos a} = \frac{1}{\cos(\tan^{-1} x)},$$

$$|H| = -\frac{1}{r} = -\cos(\tan^{-1} x).$$

The horizontal component of the H field at the point is given by:

$Hh = |H| \cos a = |H| \cos(\tan^{-1} x)$

Taking into account the directions of the current in each conductor the relative H field at the point shown in the diagram above can be found by:

$$Hh = \sum_{x=4}^{8} \cos^2(\tan^{-1} x) - \sum_{x=0}^{1} \cos^2(\tan^{-1} x) - \sum_{x=1}^{3} \cos^2(\tan^{-1} x)$$

It is also necessary to determine the vertical H fields at the points shown below:

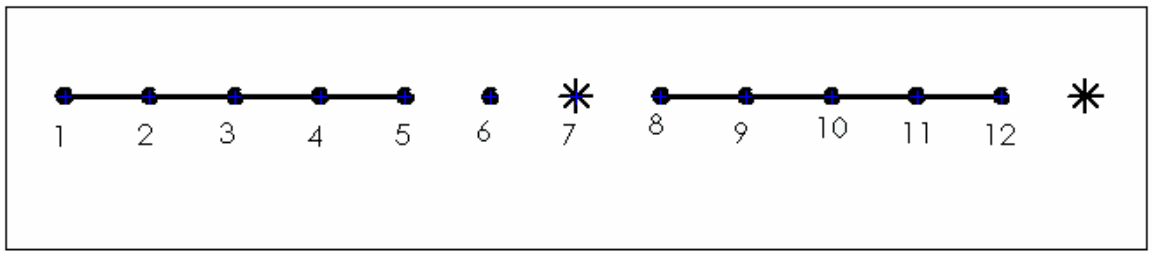

The field at point 7 can be calculated from:

$$Hv = -\sum_{x=2}^{6} \frac{1}{x} - \sum_{x=1}^{5} \frac{1}{x}$$

and the field at point 8 can be calculated from:

$$Hv = -\sum_{x=8}^{12} \frac{1}{x} + \sum_{x=1}^{5} \frac{1}{x}$$

With the fields determined at each of the points it is apparent from the symmetry of the line that the H fields on the underside of the line will equal those on the topside and that the fields surrounding the right conductor are the same as those surrounding the left conductor.

To determine the new current distribution sum the H fields around a closed contour surrounding each point. It will only be necessary to sum the H fields on the topside of the conductor. This is where an approximation has been made: The horizontal fields are considered to be in approximately the same direction for the upper shaded section of the contour and the vertically inclined fields at the ends are considered to be in the same direction as the contour for the other shaded section.

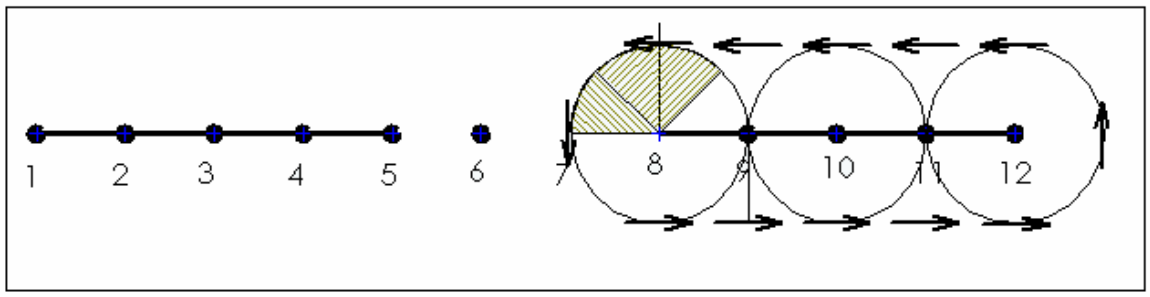

With a current now obtained for each point the next step is to normalise the currents with respect to the point with the highest current.
With this new set of currents obtained it is then required to use this set of currents in a new iteration of the above process until the current distribution converges.

Once a final current distribution has been obtained the proximity factor can be found from:

$$P = \frac{no.\_of\_points\_in\_conductor}{sum\_of\_normalised\_currents\_in\_conductor}$$

A Matlab program has been written to calculate the proximity factor. It is required for the user to enter the widths and spacing of the transmission line. Because of the crude manner in which the currents are calculated from the H field it was discovered that the best solutions are obtained when the total number of points in the model are between 10 and 20. Total number of points is given by: 2 x w + s +1.

```
% PROXIMITY - This Matlab code calculates the proximity effect in a balanced
twinline consisting of two flat plates
```

```
w=4;   %conductor width
s=5;   %spacing between conductors

I=ones(1,2*w+s+1);  %initialise point sources
for i=w+2:w+s
I(i)=0;
end

for count = 1:30    %perform 30 iterations (for convergence of current
distribution)

%Determine H fields along conductor surface

Hh=zeros(1,2*w+s+1); % Initialise array to hold H fields
Hv=zeros(1,2*w+s+1);


startpoint=w+s+1; %point on inner edge of RHS conductor

for point=startpoint:startpoint + w %sum H field contibution of LHS conductor
points for every point along RHS conductor surface.
      for i=1:1+w
      x=point-i;
      Hh(point)=Hh(point)+I(i)*(cos(atan(x)))^2;  %Horizontal Field
      %Hv(point)=Hv(point)-I(i)*cos(atan(x))*sin(atan(x));    %Vertical Field
(not used)
      end
end


for point=startpoint:startpoint + w %sum H field contibution of RHS conductor
points for every point on the left along RHS conductor surface.
      for i = startpoint:point
      x=point-i;
      Hh(point)=Hh(point)-I(i)*(cos(atan(x)))^2;  %Horizontal Field
      %Hv(point)=Hv(point)+I(i)*cos(atan(x))*sin(atan(x));    %Vertical Field
(not used)
      end
end


for point=startpoint:startpoint + w - 1 %sum H field contibution of RHS
conductor points for every point on the right along RHS conductor surface.
      for i=point+1:startpoint+w
      x=i-point;
      Hh(point)=Hh(point)-I(i)*(cos(atan(x)))^2;  %Horizontal Field
      %Hv(point)=Hv(point)-I(i)*cos(atan(x))*sin(atan(x));    %Vertical Field
(not used)
      end
end


%Determine H field present at point near inner edge of RHS conductor
centrepoint=w+s; %define this point
HCv=0;           %initialise

for i=1:1+w %Contribution from points on LHS conductor
x=centrepoint-i;
HCv=HCv-I(i)/x;
end

for i=centrepoint+1:centrepoint+1+w %Contribution from points on RHS conductor
x=i-centrepoint;
```

```
HCv=HCv-I(i)/x;
end


%Determine H field present at point near outer edge of RHS conductor
endpoint=2*w+s+2;
HEv=0;

for i=1:1+w %Contribution from points on LHS conductor
x=endpoint-i;
HEv=HEv-I(i)/x;
end

for i=endpoint-w-1:endpoint-1   %Contribution from points on RHS conductor
x=endpoint-i;
HEv=HEv+I(i)/x;
end


%Obtaining new current distribution
for i=w+s+1:2*w+s+1 %Perform Ampere's law
I(i)=abs(Hh(i));
end

I(startpoint)=I(startpoint)+abs(HCv/2); %Permorm Ampere's law at inner and outer
edges of RHS conductor
I(startpoint+w)=I(startpoint+w)+abs(HEv/2);

%Normalising current distribution
maxI=max(I);
for i=w+s+1:2*w+s+1
I(i)=I(i)/maxI;
end



% Equating LHS conductor currents to RHS conductor currents (by symmetry)
temp=zeros(1,w+1);
c=0;
for i=w+s+1:2*w+s+1
c=c+1;
temp(c)=I(i);
end

temp2=zeros(1,w+1);
for i=1:w+1
temp2(i)=temp(w+2-i);
end

for i=1:w+1
I(i)=temp2(i);
end

I   %display current distributions

end % Perform 30 iterations

%Calculate Proximity Factor
ProximityFactor=(w+1)/(sum(I)/2)
```

Appendix 3 – Matlab program for determining temperature distribution

```
%   Fourier's One Dimensional Heat Distribution Model for Temperature
Distribution in Balun/Taper
%
%   Analytical Solution using Separation of Variables to the following problem:
%     ut(x,t) = alf*uxx(x,t)   with  u(0,t) = ul   u(L,t) = ur   u(x,0) = u0
%   has solution given by
%     u(x,t) = v(x,t) + w(x)
%   where v(x,t) is the transient solution and w(x) is the steady state solution
%

%
%   getting started
      clear all,   close all
%
%   problem data
      alf = 0.000117;    % m^2/s  thermal diffusivity
      ul = 77;        % C      fixed temp at left end
      ur = 298;        % C      fixed temp at right end
      u0 = 298;         % C      initial uniform temp of bar
      L = 1;           % m      length of bar
      maxt = 50;       % max number of terms in expansion
      tol = 0.001;     % tolerance used to stop series expansion
      nfig = 0;        % figure counter
%
%   the steady state solution w(x)
      Nx = 101;   x = linspace(0,L,Nx)';   w = (ur-ul)*x/L + ul;
%
%   now v(x,t) is given as an infinite series
%   calc terms for n = 1,2,3,4,5,...,max
%   cc1 = 600*L/pi;   cc2 = 60/pi;
      for n = 1:maxt
        lam(n) = n*pi/L;  c(n) = 2*(ul-u0)*((-1)^n-1)/(n*pi)+2*(ur-ul)*(-
1)^n/(n*pi);
%   c(n) = (1/n)*(cc1*(-1)^n + cc2*((-1)^n-1));
      end
% use for plotting time snapshots
          Nt = 4;   tt = [20 40 60 80];

%   start loop over time points
      u = zeros(Nx,Nt);
      for j = 1:Nt
        t = tt(j);   cc = -alf*t;   mrerr = 1.0;   n = 0;   v = zeros(size(x));
          while mrerr > tol   &   n < maxt
            n = n+1;  vn = c(n)*sin(lam(n)*x).*exp(cc*lam(n)*lam(n));
            v = v + vn;   rerr = vn(2:Nx-1)./v(2:Nx-1);   mrerr =
max(abs(rerr));
          end
        u(:,j) = v + w;
        disp([' Needed ',num2str(n),' terms for convergence at t =
',num2str(t),' s'])
      end
%
%   plot curves of u for various times
          nfig = nfig+1;   figure(nfig)
          plot(x,u)
          axis([0 L 0 400]);
          title('Bar Temperature Distribution Over Time')
          grid,xlabel('Distance (m)'),ylabel('Temperature (K)')
          for j = 1:Nt,   gtext(['t = ',num2str(tt(j)),' s']),   end

          plot(x,u(:,1));    grid on;
```

```
          title('Bar Temperature for Initial and Final Times (Example 10.2)');
          xlabel('Distance (m)'),ylabel('Temperature (C)');
          hold off
      end
%
%   end of problem
```

Appendix 5

Determination of Noise temperature and Errors in the Noise Temperture Spreadsheet.

The spreadsheet calculates the noise temperature using equation 22. The spreadsheet applies this equation twice: once for the lower uncertainty limit of noise temperature and once for the upper uncertainty limit for noise temperature. It is evident from the graph in figure16 that by taking the upper limit of N_h and the lower limit of N_c, the intercept of the extrapolated line with the Temperature axis will move closer to the origin and will therefore indicate the lower limit of T_e. Likewise, by taking the lower limit of N_h and the upper limit of N_c, the intercept of the extrapolated line with the Temperature axis will move further from the origin and will therefore indicate the upper limit of T_e. As can be seen on the spreadsheet, there are two sections: one for the calculation of the T_e upper limit and one for the calculation of the T_e lower limit. The upper and lower limits of N_h and N_c are calculated using equation# that uses the measured power levels for hot and cold, the source reflection coefficients Gs(hot) and Gs(cold), the DUT reflection coefficient Gi and the power meter error Pe%.

The upper and lower limits of T_e are displayed at the bottom of the spreadsheet. The actual noise temperature solution is the average of the two measurements and the percentage error is calculated from the difference between the average value and the limits.